Predicting Oxygen Transfer in Hypolimnetic Oxygenation Devices

Daniel F. McGinnis

Thesis submitted to the Faculty of the

Virginia Polytechnic Institute and State University

in partial fulfillment of the requirements for the degree of

Master of Science

in

Environmental Engineering

John Little, Chair

Daniel Gallagher

Nancy Love

April 20, 2000

Blacksburg, Virginia

Keywords: Hypolimnetic oxygenation, discrete-bubble model, oxygen transfer

Predicting Oxygen Transfer in Hypolimnetic Oxygenation Devices

Daniel McGinnis

(ABSTRACT)

The purpose of this research was to apply a discrete-bubble model to predict the performance of several hypolimnetic oxygenators. The model is used to predict the oxygen transfer rate in a hypolimnetic oxygenator based on the initial bubble size formed at the diffuser. The discrete-bubble model is based on fundamental principles, and therefore could also be applied to other mass transfer applications involving the injection of bubbles into a fluid. The discrete-bubble model has been applied to a linear bubble-plume diffuser, a full-lift hypolimnetic aerator and the Speece Cone with promising results.

The first step in this research was to investigate the principals of bubble formation at a submerged orifice, bubble rise velocity and bubble mass transfer. The discrete-bubble model is then presented. The model traces a single bubble rising through a fluid, accounting for changes in bubble size due to mass transfer, temperature and hydrostatic pressure. The bubble rise velocity and mass transfer coefficients are given by empirical correlations that depend on the bubble size. Bubble size is therefore recalculated at every increment and the values for the bubble rise velocity and mass transfer coefficients are continually updated. The discrete-bubble model is verified by comparison to experimental data collected in large-scale oxygen transfer tests.

Finally, the discrete-bubble model is applied to the three most common hypolimnetic oxygenation systems: the Speece Cone, the bubble-plume diffuser, and the full-lift hypolimnetic oxygenation systems. The latter being presented by Vickie Burris in her thesis, *Hypolimnetic Aerators: Predicting Oxygen Transfer and Water Flow Rate*.

ENGINEERING SIGNIFICANCE

A discrete-bubble model is presented which describes oxygen transfer from a single bubble rising in water. The discrete-bubble model is applied to three hypolimnetic oxygenation devices: the Speece Cone, the bubble-plume diffuser, and the full-lift hypolimnetic aerator. Hypolimnetic oxygenators are designed to inject dissolved oxygen into the hypolimnion of a lake or reservoir without significantly disrupting stratification. In each device, air or oxygen bubbles are introduced into the water from a bubble diffuser. Oxygen is transferred from the bubbles into the surrounding water as the bubbles rise through the water, or as in the case of the Speece Cone, migrate down the bubble contact chamber. The amount of oxygen transferred is a function of several factors, primarily hydrostatic pressure, initial bubble size and bubble contact time. To achieve an efficient hypolimnetic oxygenator design, the dissolved oxygen goals must be properly identified, and the system should be designed to take advantage of prevailing conditions in the reservoir. The discrete-bubble model provides a means to aid the engineer in the design of an appropriate hypolimnetic oxygenator.

Because of the different characteristics and oxygenation requirements in each reservoir, one of these devices will be better suited economically and in overall performance. The bubble-plume diffuser is the simplest of these devices in both construction and operation. They are particularly suitable for deep reservoirs where there is the advantage of high hydrostatic pressure and long bubble contact time. Given the depth to the diffuser, the initial bubble size formed at the diffuser is optimized using the discrete-bubble model to design for a bubble that is not too large, which would result in decreased oxygen transfer efficiency. In the case of hydropower reservoirs, the goal is usually to increase the dissolved oxygen only in the reservoir releases. It then becomes necessary to determine the layer from which most of the water is withdrawn, or withdrawal zone, and design for a bubble size that results in the maximum amount of oxygen transfer in this layer. Frequently in hydropower reservoirs the layer below the withdrawal zone is relatively stagnant. If the bubble size is too small, substantial oxygen may be dissolved in this stagnant layer and is essentially lost. Similarly, reservoirs often exhibit a metalimnetic minimum, which is a layer of water within the metalimnion with low dissolved oxygen. In this case, the engineer will design the bubble-plume diffuser with a large enough bubble size to result in adequate oxygen transfer in the metalimnion, or given an initial bubble size, raise the diffuser allowing more oxygen transfer to occur at shallower depths in the reservoir. Other devices, such as the Speece Cone or full-lift hypolimnetic oxygenator may also be investigated as their intakes and discharges can be located at specific points, such as the metalimnion or in the withdrawal zone in a hydropower reservoir. The discrete-bubble model can also be used to evaluate the use of air or pure oxygen for the bubble-plume diffuser.

For shallow reservoirs, the bubble plume diffuser may not be feasible due to lack of bubble contact time resulting in low oxygen transfer efficiency, risk of destratification, and the possibility of entraining nutrients into the epilimnion. The full-lift hypolimnetic oxygenator may be more appropriate for these reservoirs. The full-lift hypolimnetic oxygenator uses air injected via a bubble diffuser at the base of the riser to transfer

oxygen and to induce a vertical velocity in the riser. As the bubble-water mixture rises, oxygen is transferred from the bubbles to the surrounding water. The top of the riser is exposed to the atmosphere where the bubbles exit the water, and the oxygenated water is returned to the hypolimnion via the downcomers. This minimizes disruption of the thermal density structure of the reservoir. Also, because air is used instead of oxygen, oxygen transfer efficiency is less important as air is less expensive then pure oxygen. The discrete-bubble model used in conjunction with a water flow rate model is used to design and optimize the full-lift hypolimnetic oxygenator.

The Speece Cone uses pure oxygen injected using a bubble diffuser at the top, narrow opening of the cone, or bubble contact chamber. Water is pumped simultaneously into the top of the cone resulting in a downward flow of water. The resulting downward water velocity drags the oxygen bubbles down the cone, taking advantage of the increasing hydrostatic pressure in the cone for oxygen transfer and resulting in a long bubble contact time. The Speece Cone, while the most complicated in construction and operation due to the use of a submersible pump, is the most versatile of the three hypolimnetic oxygenation devices. The Speece Cone can be effectively employed in both shallow and deep reservoirs, and for river reoxygenation. For shallower settings, the engineer can increase the hydrostatic pressure in the contact chamber using a flow control valve on the cone outlet resulting in high oxygen transfer capacity and efficiency. The engineer may also specify the location and shape of the discharge diffuser.

The area of the hypolimnion must also be considered when designing a hypolimnetic oxygenation system. For large hypolimnetic areas, a long thin rectangular bubble-plume diffuser may be used to achieve adequate oxygen distribution. However, a compact circular bubble-plume diffuser, the full-lift hypolimnetic oxygenator and the Speece Cone have higher velocity discharges and may induce sufficient mixing to transport the oxygenated water throughout the hypolimnion. The discrete-bubble model is one of several tools that should be used to design effective and efficient hypolimnetic oxygenation systems. In addition to the discrete-bubble model, a water flow rate model may also be necessary for certain hypolimnetic oxygenators. The engineer may also wish to use a two-dimensional reservoir model in conjunction with the discrete bubble model and water flow rate model to further optimize the hypolimnetic oxygenator and to investigate its impact on the reservoir.

ACKNOWLEDGEMENTS

I would like to extend my deepest gratitude to my advisor, Dr. John Little, for his support and guidance with this project. I would also like to thank him for his encouragement to publish and present research at conferences and to help me recognize and achieve my fullest potential. I would also like to thank Dr. Daniel Gallagher and Dr. Nancy Love for serving on my committee.

Gratitude is expressed to Roanoke County, VA, the Edna Bailey Sussman Fund and Tennessee Valley Authority for their financial support of this research.

I would also like to acknowledge all of those who assisted me in my research including Jeff Booth and the rest of the Roanoke County personnel. I am grateful to Dr. Robert Hoehn for getting me involved with the Spring Hollow monitoring program. I would like to express my thanks to Vickie Singleton for enthusiastically collecting data with me no matter how inclement the weather. I would like to express gratitude to my mother for her continued support and encouragement over my long college career and my best friend, Gabrielle, for always pushing me to better myself.

LIST OF TABLES

CHAPTER 2. DIFFUSED AERATION: PREDICTING GAS-TRANSFER USING A DISCRETE-BUBBLE MODEL

CHAPTER 3. BUBBLE DYNAMICS AND OXYGEN TRANSFER IN A SPEECE CONE

CHAPTER 4. HYPOLIMNETIC OXYGENATION: PREDICTING PERFORMANCE USING A DISCRETE-BUBBLE MODEL

LIST OF FIGURES

CHAPTER 1. LITERATURE REVIEW

CHAPTER 2. DIFFUSED AERATION: PREDICTING GAS-TRANSFER USING A DISCRETE-BUBBLE MODEL

CHAPTER 3. BUBBLE DYNAMICS AND OXYGEN TRANSFER IN A SPEECE CONE

CHAPTER 4. HYPOLIMNETIC OXYGENATION: PREDICTING PERFORMANCE USING A DISCRETE-BUBBLE MODEL

CHAPTER 1. LITERATURE REVIEW

Background

In the summer, lakes and reservoirs typically stratify thermally (Cole, 1994; Henry and Heinke, 1989). This is the result of solar energy warming the surface of the lake while the wind energy is not sufficient to mix this warmer, less dense water with the colder, denser bottom water (Henry and Heinke, 1989). According to Cole (1994) the stratified lake comprises three different layers, each having essentially no interaction with the other. The top layer, or epilimnion is the warmest, least dense layer and is usually of uniform temperature due to wind mixing. The bottom layer is the hypolimnion, which is characterized by cool, typically isothermal, temperature. The metalimnion is the region in the middle and is marked by rapidly decreasing temperature. Depending on the climatic conditions, lakes may remain stratified throughout the year, or they may experience mixing, or turnover, once or twice a year (Cole, 1994). These are termed oligomictic, monomictic, or dimictic lakes, respectively. Polymictic reservoirs are more rare and can turnover diurnally (Cole, 1994). Turnover typically occurs during the fall or early winter when stratification becomes unstable as the weather cools the lake surface. A wind or a storm event during this time can then generate enough energy to mix the lake. The lake will eventually become homogeneous assuming that stratification does not reoccur immediately after turnover. After turnover occurs in the fall, the lake is continually circulated and cooled until the water reaches 4 ^{o}C. If the air temperature remains cold enough, the surface water will continue cooling and become less dense then the bottom water (Henry and Heinke, 1989). Ice may also form on these lakes, rendering the lake immune to wind mixing (Cole, 1994).

Because the only sources of dissolved oxygen (DO) in lakes and reservoirs are exchange with the atmosphere and oxygen produced during photosynthesis, thermal stratification may result in substantial hypolimnetic oxygen depletion (Cole, 1994; Cooke and Carlson, 1989). DO is consumed by respiration, biochemical oxygen demand (BOD) and sediment oxygen demand (SOD) (Stefan and Fang, 1993). Low DO levels have a negative impact on cold-water fisheries, hydropower generation, and the drinking-water treatment process (Cooke et al., 1993; Mobley, 1997; Schnoor, 1996). In water-supply reservoirs, low DO may lead to the production of hydrogen sulfide, methane and ammonia, and can cause the release of phosphorus as well as reduced iron and manganese from the sediments (Cooke and Carlson, 1989; Cook et al., 1993; Schnoor, 1996). Increased phosphorus concentrations may stimulate algal growth, which exacerbates the problem since dead algae ultimately fuel additional oxygen demand. Iron, manganese and hydrogen sulfide impart undesirable color, taste, and odor to the water requiring additional treatment prior to distribution (Cooke and Carlson, 1989). The increased chlorine demand at the water treatment plant can be costly, and the additional chlorine may react with natural organic matter producing disinfection-by-products. Although there are several methods currently employed to improve water quality in stratified reservoirs (Cooke and Carlson, 1989), the process of introducing oxygen into the hypolimnion, known as hypolimnetic oxygenation, will be the focus of this research.

Hypolimnetic Oxygenation

Hypolimnetic oxygenation is the process of adding oxygen to the hypolimnion while maintaining the thermal density structure of the reservoir (Cooke et al., 1993). The goals of hypolimnetic oxygenation are to maintain high levels of DO in the hypolimnion, increase plant and fish habitat, and maintain oxic conditions at the sediments (Cooke et al., 1993). When applied in stratified reservoirs, well-designed hypolimnetic oxygenators have been shown to provide measurable increases in hypolimnetic dissolved oxygen levels (Gachter, 1995), decrease total iron, manganese, and hydrogen sulfide concentrations (McQueen and Lean, 1986; Thomas et al., 1994), and decrease blue-green algae concentrations in some cases (Kortmann et al., 1994; Gemza, 1995). Additionally, hypolimnetic oxygenation has been used to increase the dissolved oxygen levels in hydropower releases to levels of 5 or 6 mg/L (Mobley, 1997; Rayyan and Speece, 1977).

There are several types of hypolimnetic oxygen devices in use. According to Cooke and Carlson (1989), these devices are typically grouped as air injection, oxygen injection and mechanical agitation. The latter, reported as effective but inefficient, involve withdrawal of hypolimnetic water to a splash basin where it is aerated and then returned to the hypolimnion (Cooke and Carlson, 1989). Cooke and Carlson (1989) define air injection systems as the full air lift and partial air lift hypolimnetic aerators, however, this definition should be broadened to include bubble-plume diffusers using air. The oxygen systems are bubble plumes using pure oxygen injected into typically deep reservoirs in a manner to ensure high oxygen transfer (Cooke and Carlson, 1989; Rayyan and Speece, 1977; Wüest et al., 1992). Side-stream pumping withdraws water from the hypolimnion to the surface and oxygen is then added at the top of the return pipe allowing the bubbles to dissolve as they are dragged back down to the hypolimnion with the returning water (Fast et al., 1975). Destratification may be considered another method of hypolimnetic oxygenation. Air is introduced by way of a diffuser to produce enough energy to prevent the onset of, or to erode any existing stratification (Cooke and Carlson, 1989). Reaeration of the reservoir then takes place by exchange with the atmosphere (Cooke and Carlson, 1989). Possible disadvantages of destratification include the potential for the introduction of nutrients into the photic zone leading to algal blooms, increased energy costs, and warming of the hypolimnetic water which may increase the DO consumption rate and alter the ecology. This research will focus on the three principle devices used for hypolimnetic oxygenation: the Speece Cone (Speece et al., 1973), the full- or partial-lift hypolimnetic aerator (Little, 1995), and the bubble-plume diffuser (Wüest et al., 1992).

In each of these three devices, gas bubbles (either air or oxygen) are introduced into the water by means of diffusers and rise relative to the surrounding water following release. While passing through the water, gas is dissolved into the water from the bubble or stripped from the water to the bubble. The rate at which this happens depends on several factors including bubble size, partial pressure of the gas, the ambient dissolved gas concentration, and water temperature.

Speece Cone

The Speece Cone was invented by Dr. Richard Speece, who originally termed it a downflow bubble contactor (Speece et al., 1973; Thomas et al., 1994; Sanders, 1994). The device consists of a conical chamber which rest with the large diameter on the bottom of the reservoir. Water is introduced at the top of the cone where the cross sectional area is the smallest by a submersible pump and flows downward. Pure oxygen bubbles are also introduced at the top of the cone with a bubble diffuser and migrate slowly down the cone as they dissolve. The discharge is located at the base of the cone where the highly oxygenated water is introduced via a diffuser into the hypolimnion. The purpose of using the downward flow of water is that the bubbles are slowly dragged downwards in the cone with the water because the water velocity is faster then the bubble rise velocity. This allows rapid dissolution of oxygen and high oxygen transfer efficiency due to the increasing hydrostatic pressure as the bubble travels downward. Hydrodynamically, this is one of the simplest devices because the water velocity is known based on the cone geometry and the pump capacity.

Full- and Partial-Lift Hypolimnetic Aerator

There are many different types of hypolimnetic aerators in use in lakes and reservoirs (Fast and Lorenzen, 1976). Full- and partial-lift hypolimnetic aerators consist of a riser tube and one or more downcomers. The full-lift aerator extends to the water surface where it is open to the atmosphere while the partial-lift is sealed at the top, and except for the exhaust pipe, remains completely submerged. In both devices, air is bubbled into the riser at the base using a diffuser. The bubble-water mixture is less dense then the surrounding water inducing an upward velocity. As the bubble-water mixture rises, oxygen is dissolved into the water from the bubbles. At the top, the gas bubbles exit the water and the oxygenated water is returned to the hypolimnion via the downcomers. Hydrodynamically, this device is more complicated than the Speece Cone because the water velocity is a function of the volume of injected air and the more complex geometry of the device.

Bubble Plume Diffusers

The most hydrodynamically complex device is the bubble-plume diffuser. Air or typically oxygen bubbles are introduced into the bottom of the reservoir from an unconfined bubble diffuser (Cooke and Carlson, 1989; Wüest et al., 1992). The diffuser is typically a large circular diffuser (Wüest et al., 1992) or a long rectangular diffuser (Mobley, 1997). Similar to the full- and partial-lift aerators, as the bubbles are introduced into the water in the hypolimnion, the bubble-water mixture becomes less dense then the surrounding water, inducing an upward velocity. However, the plume water is not confined and surrounding water is entrained into the plume resulting in a increasing volumetric flow rate and wider plume with decreasing depth. The induced water velocity is dependent on the amount of gas introduced per unit volume if water and the thermal stratification in the reservoir. As the plume water rises, the oxygen dissolves from the bubbles traveling with the water until the plume loses its vertical momentum

and therefore velocity, and the oxygenated water falls back to the layer of neutral buoyancy (Rayyan and Speece, 1977; Wüest et al., 1992). Remaining oxygen in the bubbles continues to be transferred to the surround water until the bubbles are completely dissolved or they pass through the thermocline.

In designing these oxygenation systems, the one factor the engineer has control over, and which will most strongly determine the performance of the system, is the initial bubble size formed at the diffuser. If the initial bubble size is known, then the bubble can be tracked as it rises through the device accounting for changes in bubble volume due to mass transfer into and out of the bubble, hydrostatic pressure changes and temperature changes. To calculate the rate of gas transfer the bubble rise velocity and mass transfer coefficient must be known; both of which are functions of bubble size. The bubble rise velocity partially determines the time for mass transfer between the bubble and the water to take place. The mass transfer coefficient is used to determine how rapidly oxygen and nitrogen are transferred across the liquid water interface of the bubble. The induced water velocity is also an important parameter in determining the bubble contact time, but is not the focus of the current research.

Although many models have been developed for these devices (Fast and Lorenzen, 1976; Ponoth and McLaughlin, 2000; Pöpel and Wagner, 1991; Schladow, 1993; Tsang, 1991) the first comprehensive model that included the effect of oxygen transfer based on fundamental principals was developed by Wüest et al. (1992). In that analysis, correlation equations were developed from previously published data relating bubble rise velocity and the mass transfer coefficient to bubble radius. The relationships were then used to predict oxygen transfer within the rising buoyant plume. This discrete-bubble approach has subsequently been shown to hold considerable promise for predicting the performance of full-lift hypolimnetic aerators (Burris and Little, 1998) and the Speece Cone (McGinnis and Little, 1998).

Several previous researchers have used a similar approach, but neglected the changes in the bubble size due to mass transfer into and out of the bubble and hydrostatic and thermal changes as the bubble travels through the fluid. Typically, the overall average mass transfer coefficient for a particular device is measured (Motarjemi and Jameson, 1977; Ponoth and McLaughlin, 1999; Pöpel and Wagner, 1991; Speece and Rayyan, 1973; Wagner and Pöpel, 1996; Wagner et al., 1998). One model was found which accounts for changes in bubble volume due to hydrostatic pressure (Pöpel and Wagner, 1994). And finally, a single-bubble model for ozone was found which accounts for changes in bubble size due to hydrostatic pressure changes and mass transfer effects, but the author determined that changes in the mass transfer coefficient and bubble rise velocity were negligible in the experiments (Bin, 1995).

Bubble Formation

The major factors affecting the initial bubble size formed at the diffuser are the orifice size, gas momentum, and chamber volume (Clift et al., 1978; Marmur and Rubin, 1976; Miyahara and Takahashi, 1984). The chamber volume is defined as the volume of the gas contained below the orifice, although at high gas flow rates, the effect of the chamber volume is diminished (Davidson and Amick, 1956; Miyahara and Takahashi, 1984). Minor factors affecting bubble formation are the horizontal and vertical flow of water past the orifice, depth, temperature, the angle of the orifice, the wake effects from previously formed bubbles, boundary effects, and bubble coalescence (Bischof et al., 1994; Clift et al., 1979; Marmur and Rubin, 1976; Tsuge et al., 1992). At low gas flow rates, the effect of gas momentum becomes negligible, and the bubble volume is simply a function of buoyancy and surface tension (Hayes et al., 1959). Assuming that air is pumped into the gas chamber at a low flow rate, the pressure within the chamber can be calculated using Laplace's equation (Hayes et al., 1959)

$$P_i = P + \frac{2\sigma}{r} \qquad (1)$$

where P_i is the pressure within the bubble and the gas chamber (assumed to be equal), P is the hydrostatic pressure just above the orifice, σ is the surface tension of the water, and r is the radius of curvature of the bubble forming at the orifice. When the radius of the bubble approaches infinity, that is, the air-water interface is level with the orifice and the top surface of the gas chamber, then the pressure in the chamber is equal to the surrounding hydrostatic pressure (Adamson, 1982).

As more gas is pumped into the chamber, the radius of curvature of the bubble starts to decrease as the bubble size increases. As shown by Equation 1, there is a corresponding increase in pressure within the chamber and the developing bubble. The growth process continues to the point at which the buoyant force, F_b, exerted on the bubble is equal and opposite to the force due to surface tension, F_σ (Pinczewski, 1980). After this stage, the buoyant force overcomes the force due to surface tension (Pinczewski, 1980). The buoyant force causes the bubble to act as a pump and the bubble can draw additional air from the gas chamber. The bubble continues to grow until it necks and detaches. Necking is a result of the motion of the surrounding fluid which is caused by the bubble growth (Hooper, 1986). The pressure variations in the chamber decrease as the chamber volume is increased because of the excess amount of gas that occurs in the chamber between bubble formations (Davidson and Amick, 1956). This is known as the constant pressure or varying flow condition (Clift et al., 1978; Marmur and Rubin, 1976; Satyanarayan et al., 1969). The excessive amount of gas that exists in the chamber results in the formation of a larger bubble than would occur with a smaller chamber volume (Clift et al., 1978). Conversely, the constant flow condition is when the chamber volume is small, the pressure can decrease significantly when the bubble is formed, resulting in a smaller bubble volume (Clift et al., 1978; Satyanarayan et al., 1969). At higher flow rates this effect begins to diminish because the gas flow entering the chamber

will more rapidly replace that which is drawn out, causing a constant pressure to be maintained (Hayes et al., 1959).

As the gas flow rate is increased, the gas momentum acting on the forming bubble must also be considered (Pinczewski, 1980). The volume of the bubble reaches a maximum for a given orifice as the gas flow rate is further increased, after which the momentum will become powerful enough to shear the bubble away from the orifice (Davidson and Amick, 1956).

Constant Frequency vs. Constant Volume

Bubble formation at an orifice can be classified in two ranges, the constant volume range and the constant frequency range (Hayes et al., 1959; Marmur and Rubin, 1976). The constant volume range occurs at lower gas flow rates when the primary factors affecting the bubble volume are orifice size and chamber volume (Hayes et al., 1959). Because both remain constant, the bubble volume will remain constant and the increasing gas flow rate results only in an increasing frequency of bubble formation (Hayes et al., 1959). The breakpoint is defined by Hayes et al. (1959) as the point at which the transition between constant bubble volume and constant frequency begins to occur. The breakpoint is the point at which the gas momentum begins to increase the bubble volume, and the frequency of bubble formation becomes essentially constant (Hayes et al., 1959). If the flow rate is increased beyond a certain point, constant bubble volume formation is once again obtained, however, bubbles will begin to form at the orifice simultaneously in sets of two or greater (Davidson and Amick, 1956; Marmur and Rubin, 1976). This is a highly unstable range of bubble formation and may increase the likelihood of coalescence (Davidson and Amick, 1956; Tsuge et al., 1992).

Bubble formation from diffusers: Bischof et al. (1994)

Bischof et al. (1994) suggest a simple equation for predicting the diameter of a bubble produced at a submerged diffuser orifice. The model is based on an equilibrium force balance calculation on a bubble at the orifice (Bischof et al., 1994). For water at a temperature of 20^{o}C the bubble diameter formed is expressed as a simple function of orifice diameter,

$$D = 3.236 D_o^{1/3} \tag{2}$$

In addition to this equation, Bischof et al. (1994) lists the following criteria to consider when designing a diffuser. The maximum frequency of bubble formation that can occur from a single orifice on the diffuser is

$$f_{max} = \frac{u_b}{D} \tag{3}$$

where u_b is the rise velocity of the bubble. Therefore, the theoretical maximum frequency of bubble formation from a single orifice on the diffuser occurs when one

bubble follows another without any distance between them (Bischof et al., 1994). So, the maximum gas flow through the orifice can be written as

$$Q_{max} = f_{max} V \tag{4}$$

To avoid bubble coalescence, the design frequency should be no greater than 2/3 of the theoretical maximum frequency (Bischof et al., 1994):

$$f = \frac{2}{3} f_{max} \tag{5}$$

The absolute maximum number of orifices that can exist on a diffuser surface is (Bischof et al., 1994)

$$N_{0\,max} = \frac{A}{D^2} \tag{6}$$

where A is the surface area of the diffuser. This would obviously be too dense a configuration, so a parameter *a* is introduced which represents the minimum distance between two orifices, and is some multiple of the bubble diameter (Bischof et al., 1994). The number of orifices then becomes

$$N_0 = \left[2 + \mathrm{INT}\left(\frac{N_{0\,max}^{1/2} - 2 - a/D}{a/D + 1} \right) \right]^2 \tag{7}$$

The gas flux is defined as

$$Q_F = \frac{\pi}{9} f_{max} D^3 N_0 \tag{8}$$

and the maximum gas flux per unit surface is

$$\frac{Q_{F\,max}}{A_{max}} = \frac{\pi}{6} u_b \tag{9}$$

Bischof et al. (1994) suggests that a = 3D is sufficient to prevent coalescence for the condition of A >> D. This factor is correlated (Bischof et al., 1994) to give the following equation for gas flux per unit area to avoid coalescence

$$\frac{Q_{F\,max}}{A_{max}} \approx \frac{1}{2} u_b \tag{10}$$

The rise velocity, u_B, should include the vertical water flow past the orifice.

Bubble Rise Velocity

The terminal bubble rise velocity is an important factor in determining the mass transfer efficiency as this partly determines the bubble contact time in the water. The primary factors influencing the terminal bubble rise velocity are bubble size, fluid viscosity, density and surface tension (Haberman and Morton, 1956; Jamialahmadi et al., 1994). Bubble size determines which of these factors dominates (Haberman and Morton, 1956). However, in a study of bubble motion performed by Haberman and Morton (1953) they conclude that the terminal rise velocity of a bubble could not be predicted by the physical properties of the fluid alone, including viscosity, surface tension and density. Additionally, surfactants have also been shown to influence bubble rise velocity (Haberman and Morton, 1956; Ponoth and McLaughlin, 1999).

Bubbles smaller then 1 mm in radius rising in tap water behave as rigid spheres (Figure1) (Haberman and Morton, 1953). In this range there is no movement, or slip of the bubble surface, no internal circulation in the bubbles, and the bubble is essentially spherical (Jamialahmadi et al., 1994; Haberman and Morton, 1953; Ponoth and McLaughlin, 1999). Internal circulation in the rigid bubble is inhibited due to surfactants on the bubble surface which reduce surface tension (Ponoth and MacLaughlin, 1999). As the small bubble rises through a fluid, surfactants adsorbed to the surface of the bubble are swept to the back of the bubble resulting in an inhibition of surface motion caused by the tangential stress resulting from this phenomena (Ponoth and MacLaughlin, 1999). However, Haberman and Morton (1953) indicate that the molecules on the bubble surface travel with the bubble resulting in the bubble behaving as a rigid sphere. Therefore, as shown in Figure 1, the bubbles behaving as a rigid sphere follow Stoke's Law (Haberman and Morton, 1953). The effects of surfactants on the rising bubble can be seen by comparing bubbles of 0.6 mm radius rising in tap water versus distilled water (Figure 1). The discrepancy in terminal rise velocities for the distilled and tap water indicates that the presence of impurities on the bubble surface cause the bubble to behave as a rigid sphere, increasing the drag (Haberman and Morton, 1953). Furthermore, when the concentration of surfactants is very high, the repulsion of the particles also needs to be considered (Ponoth and McLaughlin, 1999).

For small bubbles, the surface tension makes the bubble spherical resulting in a minimal surface area (Haberman and Morton, 1953). As the bubble diameter increases, the shear force exerted on the bubble surface becomes strong enough to lessen the effect of the surface forces (Haberman and Morton, 1953). This results in a flattening of the bubble into an ellipsoid, which in turn results in higher drag forces (Haberman and Morton, 1953; Pöpel and Wagner, 1991). The drag force exerted on the bubble continues to increase with increasing bubble diameter until a constant drag coefficient is reached (Haberman and Morton, 1953). Figure 1 suggests this constant drag coefficient occurs for bubbles of 5 mm radius and larger in water. The transitional zone from a spherical to elliptical bubble is the point at which the bubble begins to behave as a fluid particle rather than a rigid sphere (Haberman and Morton, 1953). At this point, circulation begins to occur within the bubble and surface tension, viscosity and density dominate motion (Haberman and Morton, 1953). Also, shear forces exerted on the bubble in the elliptical

and spherical cap range are strong enough to prevent the accumulation of particles on the bubble surface (Haberman and Morton, 1953).

Bubble Rise Velocity Correlation

Jamialahmadi et al. (1994) propose a correlation for the terminal rise velocity based on Stoke's Law combined with a surface wave analogy. This correlation is reported to better represent the mechanics of bubble motion (Jamialahmadi et al., 1994).

The terminal rise velocity of a spherical particle or rigid bubble is defined as

$$u_b^{sp} = \frac{1}{18}\frac{\rho_G - \rho_L}{\mu_L} gD^2 \tag{11}$$

however, as stated previously, this can only be applied to a rigid bubble. Jamialahmadi et al. (1994) state that larger bubbles begin to oscillate and these oscillations, according to Lamb (1945), can be considered similar to the motion of a wave traveling in an ideal fluid. The wave velocity is given by Lamb (1945) as

$$u^1 = \left(\frac{g\lambda}{2\pi}\right)^{1/2} \tag{12}$$

where λ is the wavelength or

$$\lambda = \frac{8\pi x^2}{gt^2} \tag{13}$$

where x is the distance between the wave profiles and t is the time the surface is occupied by the particular wave-system (Lamb, 1945). However λ is reported to have a value of the circumference of a sphere with a volume equivalent to that of the bubble (Jamialahmadi et al., 1994). The influence of surface tension must be included for large bubbles (Lamb, 1945). Therefore, the velocity of the wave due to capillarity, which are discontinuous fluid pressures at the surface of the air-water interface of the bubble (Lamb, 1945), is (Jamialahmadi et al., 1994)

$$u^2 = \left(\frac{2\pi\sigma}{\lambda(\rho_L + \rho_G)}\right)^{1/2}. \tag{14}$$

Jamialahmadi et al. (1994) combine equations 12 and 14 to account for both wave mechanisms and substitute 2π for λ to obtain

$$u^w = \left(\frac{2\sigma}{D(\rho_L + \rho_G)} + \frac{gD}{2} \right)^{1/2} \tag{15}$$

Equations 32 and 36 are now combined to form a correlation equation to predict the terminal rise velocity for the entire range of bubble sizes (Jamialahmadi et al., 1994)

$$u_b = \frac{u_b^{sp} u^w}{\sqrt{\left(u_b^{sp}\right)^2 + \left(u^w\right)^2}}. \tag{16}$$

Mass Transfer

Interphase mass transfer is the transfer of materials across a boundary, such as the air-water interface (Weber and DiGiano, 1996). The transfer of oxygen from a bubble to the surrounding water is focused on here, as it is of interest for hypolimnetic oxygenation systems. The primary factors affecting the mass transfer rate for an individual bubble are the bubble size, internal gas circulation, bubble rise velocity and surfactants (Ponoth and McLaughlin, 1999). While several models are available to predict the mass transfer coefficient, most of them are difficult to use and reported inaccurate in the literature over the entire range of bubble sizes (Mortarjemi and Jameson, 1978; Weber and DiGiano, 1996). Currently, a simple set of correlation equations developed by Wüest et al. (1992) are used to estimate the mass transfer coefficient for oxygen and nitrogen for a single bubble as a function of bubble size (Figure 2). These equations are based on two linear fits to the data obtained by Motarjemi and Jameson (1977).

Bubble size is the most important factor in determining the rate of mass transfer. Smaller bubbles, while having a longer contact time also have a smaller mass transfer coefficient (Figure 2). This is due to the fact that, as stated previously, the bubble behaves as a rigid sphere resulting in little to no internal circulation (Motarjemi and Jameson, 1977). No internal circulation results in oxygen or other gas molecules being transferred from the center of the bubble to the interface primarily by diffusive transport which is much slower then dispersive transport (Weber and DiGiano, 1996), which is present in a bubble with high internal circulation. Mass transfer from smaller bubbles is also more prone to interference due to surface active agents as these immobilize the bubble surface and inhibit molecular diffusion (Motarjemi and Jameson, 1977). Motarjemi and Jameson (1977) recommend that small bubbles less then 0.025 mm in radius be avoided for this reason. As indicated in Figure 2, the mass transfer coefficient rises steadily to a maximum at a bubble diameter of approximately 2 mm. This suggests that the bubble begins to circulate internally in this region (Motarjemi and Jameson, 1977). The surface of very large bubbles tends to move freely and be less affected by surface impurities resulting in a higher mass transfer coefficient (Motarjemi and Jameson, 1997). However, the surface area to volume ratio is smaller for large bubbles, resulting in a longer time for the oxygen molecules to transfer from the gas to liquid phase.

Research suggests that a high water velocity past a bubble may increase the mass transfer coefficient (Jun and Jain, 1993). This may be due in part to the increase in turbulence resulting in a decrease of the concentration gradient in both the liquid and gas phase (Weber and DiGiano, 1996), as well as a more freely moving bubble surface and increased internal gas circulation.

Significant mass transfer may also occur as the bubble forms at the diffuser (Clift et al., 1978). According to Clift et al. (1978) the higher mass transfer is due to high internal circulation during bubble formation as well as a new, contaminant-free bubble surface. Also, during bubble release, mass transfer rates may be increased due to oscillations, bubble acceleration and high internal gas circulation (Clift et al., 1978).

Nomenclature

a	minimum distance between two orifices on a diffuser (m)
A	surface area of the diffuser (m^2)
D	bubble diameter (m)
D_o	orifice diameter (m)
f	frequency of bubble formation (s^{-1})
g	acceleration due to gravity (m s^{-2})
N_o	number of orifices on a diffuser (-)
Q	volumetric gas flow rate through an orifice (m^3 s^{-1})
t	time (s)
u	rise velocity (m s^{-1})
V	bubble volume (m^3)
x	distance between wave profiles (m)

Greek Symbols

λ	wave length (m)
μ	dynamic viscosity (N s m^{-2})
ρ	density (kg m^{-3})
σ	surface tension (N m^{-1})

Subscripts

b	bubble
G	gas
L	liquid

Superscripts

1	oscillation
2	capillarity

sp	spherical bubble
w	fluid bubble

References

Adamson, A. W., *Physical Chemistry of Surfaces,* 4th ed., 664 pp., J. Wiley, New York, NY 1982.

Bin, A. K., Application of a single-bubble model in estimation of ozone transfer efficiency in water, *Ozone Science & Engineering*, 17, 469-484, 1995.

Bischof, F., F. Durst, M. Hofken and M. Sommerfeld, Theoretical considerations about the development of efficient aeration systems for activated sludge treatment, *Aeration Technology: ASME*, 187, 27-38, 1994.

Burris, V. L., J. C. Little, Oxygen transfer in a hypolimnetic aerator, *Water Sci. Technol.,* 37, 2, 1998.

Clift, R., J. R. Grace and M. E. Weber, *Bubbles, Drops, and Particles,* Academic Press, New York, NY, 1978.

Cole, G. A., *Textbook of Limnology*, 4th ed., 412 pp., Waveland Press, Inc., Prospect Heights, IL, 1994.

Cooke, G. D. and R. E. Carlson, *Reservoir Management for Water Quality and THM Precursor Control*, 387 pp., AWWA Research Foundation, Denver, CO, 1989.

Cooke, G. D, E. B. Welch, S. A. Peterson and P. R. Newroth, *Restoration and Management of Lakes and Reservoirs*. 2nd edn, Lewis Publishers, Boca Raton, 1993.

Davidson, L. and E. H. Amick, Jr., Formation of gas bubbles at horizontal orifices, *A. I. Ch. E. Journal,* 2, 3, 337-342, 1956.

Fast, A. W., W. J. Overholtz and R. B. Tubb, Hypolimnetic Oxygenation Using Liquid Oxygen, *Water Resources Research*, 11, 2, 294-299, 1975.

Gachter, R., Ten years experience with artificial mixing and oxygenation of prealpine lakes, *Lake and Reserv. Manage.*, 11, 141, 1995.

Gemza, A., Some practical aspects of whole lake mixing and hypolimnetic oxygenation. Ecological impacts of aeration on lakes and reservoirs in southern Ontario, *Lake and Reserv. Manage.*, 11, 141, 1995.

Haberman, W. L. and R. K. Morton, An experimental study of bubbles moving in liquids, *Proc. Am. Soc. Civ. Eng., 80,* 379-427, 1954.

Hayes, W. B. III, B. W. Hardy and C. D. Holland, Formation of gas bubbles at submerged orifices, *A.I.Ch.E Journal,* 5, 3, 319-324, 1959.

Henry, J. G. and G. W. Heinke, *Environmental Science and Engineering,* 728 pp., Prentice-Hall, Inc., London, 1989.

Hooper, A. P., A study of bubble formation at a submerged orifice using the boundary element method, *Chemical Engineering Science*, 41, 7, 1879-1890, 1986.

Jamialahmadi, M., C. Branch and J. Müller-Steinhagen, Terminal rise velocity in liquids, *Trans IchemE*, 72, Part A, 1994.

Jun, K. S. and S. C. Jain, Oxygen transfer in bubbly turbulent shear flow, *J. Hyd. Eng., 119,* (1), 21-36, 1993.

Kortmann, R. W., G. W. Knoecklein and C. H. Bonnell, Aeration of stratified lakes: Theory and practice, *Lake and Reserv. Manage.*, 8, 99-120, 1994.

Lamb, H., *Hydrodynamics,* 6th ed., 738 pp., Dover Publications, New York, 1945.

Little, J. C., Hypolimnetic aerators: Predicting oxygen transfer and hydrodynamics, *Wat. Res*., *29*, 2475-2482, 1995.

Marmur, A. and E. Rubin, A theoretical model for bubble formation at an orifice submerged in an inviscid liquid, *Chemical Engineering Science*, 31, 453-463, 1976.

McGinnis, D. F. and Little, J. C. (1998). Bubble dynamics and oxygen transfer in a Speece Cone. *Water Science & Technology*, **37** (2) 285-292.

McQueen, D. J. and D. R. S. Lean, D.R.S., Hypolimnetic aeration: An overview, *Water Poll. Res. J. Can*., 21, 205-217, 1986.

Miyahara, T. and T. Takahashi, Bubble volume in single bubbling regime with weeping at the orifice, *Journal of Chemical Engineering of Japan*, 17, 6, 597-602, 1984.

Mobley, M. H., TVA Reservoir Aeration Diffuser System, TVA Technical Paper 97-3, *ASCE Waterpower '97*, Atlanta, GA, August 5-8, 1997

Motarjemi, M. and G. J. Jameson, Mass transfer from very small bubbles - The optimum bubble size for aeration, *Chemical Engineering Science, 33,* 1415-1423, 1978.

Pinczewski, W. V., The formation and growth of bubbles at a submerged orifice, *Chem. Eng. Sci.,* 36, 405-411, 1980.

Ponoth, S. S. and J. B. McLaughlin, Numerical simulation of mass transfer for bubbles in water, *Chemical Engineering Science*, 55, 1237-1255, 2000.

Pöpel, H. J. and M. Wagner, Prediction of oxygen transfer from simple measurements of bubble characteristics, *Wat. Sci. Tech*., *23*, 1941-1950, 1991.

Rayyan, F. and R. E. Speece, Hydrodynamics of bubble plumes and oxygen absorption in stratified impoundments, *Prog. Wat. Tech*., 9, 129-142, 1977.

Satyanarayan, A., R. Kumar and N. R. Kuloor, Studies in bubble formation – II: Bubble formation under constant pressure conditions, *Chemical Engineering Science*, 24, 749-764, 1969.

Sanders, J. O. Jr., Camanche hypolimnetic oxygenation demonstration project, East Bay Municipal Utility District, Oakland, California, 1994.

Schladow, S. G., Lake destratification by bubble-plume systems: Design methodology, *Jour. Hyd. Eng.*, 119, 350-368, 1993.

Schnoor, J. L., *Environmental Modeling: Fate and Transport of Pollutants in Water, Air and Soil*, John Wiley & Sons, Inc., New York, 1996.

Speece, R. E., Rayyan, F. and G. Murfee, Alternative considerations in the oxygenation of reservoir discharges and rivers. In: *Applications of commercial oxygen to water and wastewater systems*. R. E. Speece and J. F. Malina, Jr. (Ed.), Center for Research in Water Resources, Austin Texas, 342 – 361, 1973.

Stefan, H. G. and X. Fang, Dissolved oxygen model for regional lake analysis, *Ecological Modelling*, 71, 37-68, 1994.

Thomas, J. A., W. H. Funk, B. C. Moore and W. W. Budd, Short term changes in Newman Lake following hypolimnetic aeration with the Speece Cone, *Lake and Reservoir Management*, 9, 1, 111 – 113, Extended Abstract of a paper presented at the 13th International Symposium of the North American Lake Management Society, Seattle, WA, Nov. 29 - Dec. 4, 1993, 1994.

Tsang, G., Theoretical investigation of oxygenating bubble plumes, in *Air-Water Mass Transfer-Selected Papers from the Second International Symposium on Gas Transfer at Water Surfaces*, pp. 715-727, ASCE, New York, NY, 1991.

Tsuge, H., Y. Nakajima and K. Terasaka, Behavior of bubbles formed from a submerged orifice under high system pressure, *Chem. Eng. Sci.,* 47, 13/14, 3273-3280, 1992.

Wagner, M. R. and H. J. Pöpel, Surface active agents and their influence on oxygen transfer, *Wat. Sci. Tech*., 34, 3-4, 249-256, 1996.

Wagner, M. R., H. J. Pöpel and P Kalte, Pure oxygen desorption method – A new and cost-effective method for the determination of oxygen transfer rates in clean water, *Wat. Sci. Tech*., 38, 3, 103-109, 1998.

Weber, W. J. Jr. and F. A. DiGiano, *Process Dynamics in Environmental Systems,* 943 pp., John Wiley & Sons, Inc., New York, NY, 1996.

Wüest, A., N. H. Brooks and D. M. Imboden, Bubble plume modeling for lake restoration, *Water Resources Research,* 28, 12, 3235-3250, 1992.

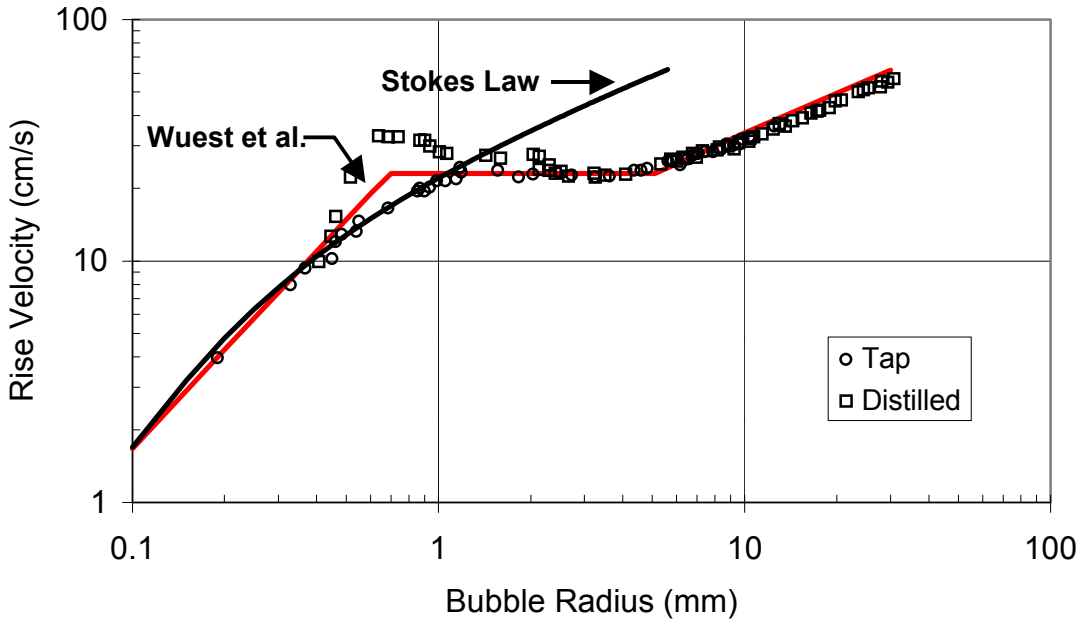

Figure 1. Terminal bubble rise velocity as a function of bubble radius. Data from Haberman and Morton, 1956.

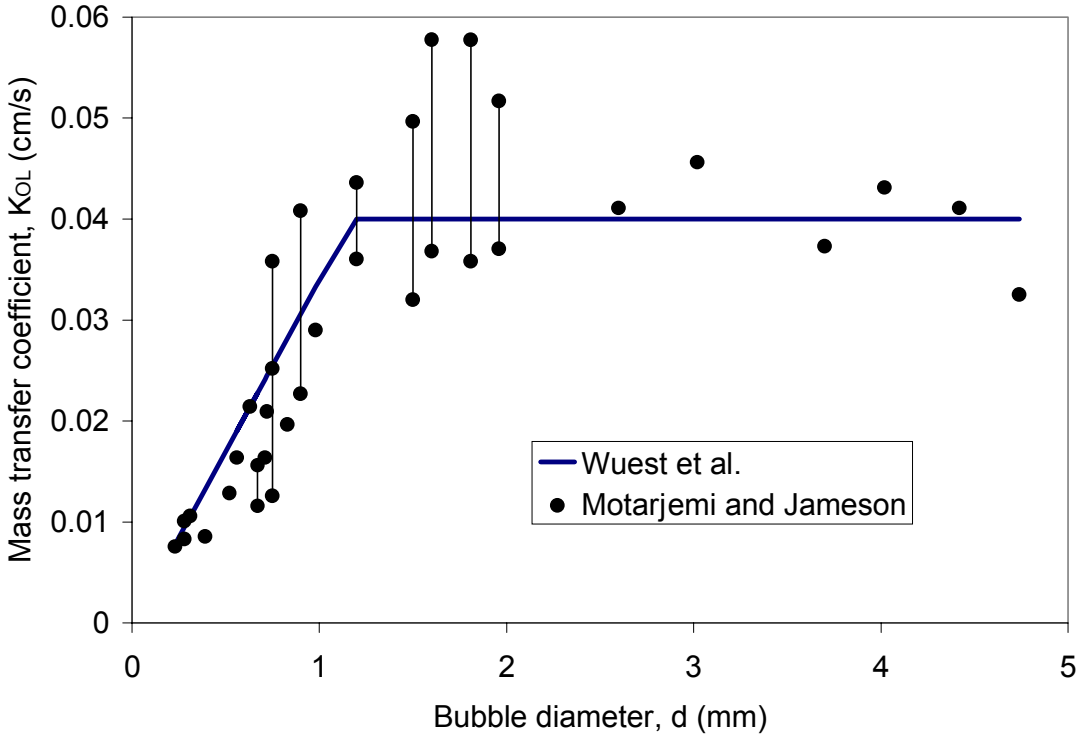

Figure 2. Mass transfer coefficient for a single bubble as a function of bubble diameter. Data from Motarjemi and Jameson, 1978.

CHAPTER 2. DIFFUSED AERATION: PREDICTING GAS-TRANSFER USING A DISCRETE-BUBBLE MODEL

DANIEL F. MCGINNIS AND JOHN C. LITTLE

Department of Civil Engineering, Virginia Polytechnic Institute and State University, Blacksburg, Virginia 24061-0105, USA

ABSTRACT

A model is presented that predicts oxygen transfer based on knowledge of the initial bubble size formed at the diffuser. The model relies on fundamental principals to track a single bubble rising in a fluid to predict oxygen transfer, and accounts for changes in the bubble volume due to mass transfer, temperature, and hydrostatic pressure changes. The model is expanded to account for multiple bubbles formed at the diffuser. This paper also demonstrates that the Sauter-mean diameter can be used rather than the bubble size distribution to represent the mass transfer of the bubble swarm. The model is verified with laboratory data with good success. This process model will aid in the design and optimization of hypolimnetic oxygenation systems, or other diffused gas systems.

Introduction

Raw water quality is an important consideration for treatment plant operators. Ever tightening drinking water standards have forced treatment facilities to focus on water resource protection and management rather than improved technologies to reach increasingly difficult treatment goals (Cooke and Carlson, 1989). One method used to maintain raw water quality in reservoirs is hypolimnetic oxygenation (Cooke and Carlson, 1989). During periods of warm weather lakes thermally stratify and form three distinct layers (Cole, 1994). The surface water warms, becoming less dense than the water below. This surface layer, or epilimnion, is where most algal activity occurs, and typically has high levels of dissolved oxygen. Immediately beneath the epilimnion is a region of rapidly decreasing temperature, or metalimnion. The bottom layer in a stratified lake is the hypolimnion, which is cold, dense, and usually isothermal.

During periods of thermal stratification dissolved oxygen (DO) is consumed in the hypolimnion through such processes as respiration, sediment oxygen demand, and biochemical oxygen demand (Stefan and Fang, 1993). Because the hypolimnion is not in contact with the atmosphere, the primary source of oxygen, dissolved oxygen levels may become depleted (Cole, 1994). Water quality concerns associated with an anoxic hypolimnion include the release of reduced iron and manganese from the sediment and production of hydrogen sulfide (Cooke and Carlson, 1989). These require additional treatment to remove and are aesthetically unpleasing to the consumer. Nitrogen and phosphorus may be liberated from the sediments causing additional algal growth which

lead to taste and odor problems, clog filters, and can increase trihalomethane (THM) concentrations during disinfection (Cooke and Carlson, 1989).

One method commonly employed to improve water quality in stratified reservoirs is hypolimnetic oxygenation (Cooke and Carlson, 1989). Properly designed hypolimnetic oxygenators add oxygen to the hypolimnion without destratifing the lake or reservoir. Undersizing an oxygenation system or employing an inappropriate design can also be detrimental to a reservoir (Cooke and Carlson, 1989). The three most commonly used hypolimnetic oxygenation systems are the Speece Cone, the full- or partial-lift hypolimnetic aerator, and the bubble-plume diffuser (Little, 1995). Selection of an appropriate device depends on the morphological features of the reservoir, as well as the dissolved oxygen depletion rate. A well designed oxygenation system takes advantage of reservoir conditions, such as depth, while meeting the oxygen demand, ensuring good efficiency, and achieving proper oxygen distribution. With proper design and careful monitoring, an oxygenation system is a valuable first stage in the water treatment process.

The initial bubble size formed at the diffuser is the most important consideration in determining the performance of hypolimnetic oxygenation systems. It is important that the bubble is not too large, resulting in unutilized oxygen and higher operating costs. If the bubble volume is too small, mass transfer may be inhibited by the adsorption of particles to the surface (Motarjemi and Jameson, 1978). Knowledge or specification of the initial bubble size formed at the diffuser and tracking the bubble as it travels through the water using the discrete-bubble model is a useful design tool for hypolimnetic oxygenators. This discrete-bubble model has also been shown to hold considerable promise for predicting the performance of full-lift hypolimnetic aerators (Burris and Little, 1998) and the Speece Cone (McGinnis and Little, 1998). The discrete bubble model was first adopted by Wüest et al. (1992) to predict oxygen transfer in their bubble-plume model, but has not yet been independently verified.

Experimental Methods

Mass Transfer Tests

The discrete-bubble model was verified by oxygen transfer tests conducted in a 14-m high by 2-m diameter tank using the TVA "soaker hose" diffuser. The porous "soaker hose" is used by TVA in their bubble-plume line diffuser, shown schematically in Figure 1 (Mobley, 1997). A 1.5-m section of diffuser using 6.4-mm diameter "soaker hose" was located 0.6-m above the floor of the tank. The dissolved oxygen in the water was removed using 10 mg/L sodium sulfite per 1 mg/L of dissolved oxygen, with 5 g of cobalt chloride as a catalyst. The tests were performed at air flow rates of 0.46, 0.73, and 3.1 $Nm^3\ h^{-1}$, where Nm^3 denotes 1 m^3 of gas at 1 bar and 0^oC (Wüest et al., 1992). The air flow rate was measured using a rotameter, which was calibrated using the measured change in weight of the gas tank with time. Dissolved oxygen and temperature data were collected using three multiprobe sondes placed in the tank at depths of 3, 8, and 12 meters

below the water surface. One of the sondes was manufactured by YSI and the other two were Hydrolabs. Each mass transfer test was run until the dissolved oxygen concentration approached saturation with respect to the surface.

Bubble Size Measurements

Photographs of the bubble swarm were taken through the bottom porthole of the tank. A 30-cm section of soaker hose was located 50 cm above the bottom the tank, and was positioned 9 cm from the porthole. A graduated scale (2-mm resolution) was positioned behind the soaker hose. Photographs were taken at four different air flow rates, and a duplicate test was performed at approximately the same air flow rates and water depth. The photographs were then digitized using a color scanner. Twenty bubbles were randomly selected to determine the average bubble diameter in each photograph. Previous research suggests that a total of 20 bubbles will provide a representative sample (Ashley et al., 1990; Ashley et al., 1991; Chen et al., 1993). Both the horizontal and vertical axis of each bubble were measured in Microsoft Photo Editor. The bubbles were typically not spherical, and were usually slightly larger in the horizontal axis. The spherical surface area of the bubble, A, is

$$A = \frac{\pi d_x d_y}{4} \quad (mm^2) \tag{1}$$

where d_x and d_y are the bubble diameters in the horizontal and vertical axis, respectively. The equivalent spherical diameter is

$$d = \sqrt{\frac{4A}{\pi}} \quad (mm) \tag{2}$$

Because of the complexity of solving the discrete-bubble model using the bubble size distribution, the Sauter-mean diameter is used as the average bubble size. The Sauter-mean diameter accounts for the surface area to volume ratio of the bubble swarm, giving more weight to larger bubbles (Orsat et al., 1993). The Sauter-mean diameter is therefore more representative for mass transfer than the mean bubble diameter and is defined (Orsat et al., 1993) as

$$d_{3,2} = \frac{\sum_{i=1}^{n} d_i^3}{\sum_{i=1}^{n} d_i^2} \quad (mm) \tag{3}$$

where d_i is the equivalent spherical bubble diameter (mm) and n is the number of bubbles in the sample. The bubble measurement procedure was carried out at water depths of 7 and 14 m to determine the effect of water depth on the bubble size formed at the diffuser.

Discrete-Bubble Model

Model Assumptions

The following assumptions are based on those initially used by Wüest et al. (1992):

- The bubbles rise in plug flow;
- The bubbles produced by the diffuser are the same size;
- Bubble coalescence is neglected, and the number of bubbles formed at the diffuser per unit time, or bubble number flux, is constant;
- Mass transfer of gasses other than nitrogen and oxygen is neglected;
- The water and gas temperatures are equal and constant;
- The water in the tank is well-mixed;
- Surface reaeration is neglected.

Model Development

The discrete bubble model, first adopted by Wüest et al. (1992), is developed assuming a discrete bubble rising in plug flow through well-mixed water. The flux of gas across the surface of the bubble is

$$J = K_L (C_s - C) \quad (\text{mol m}^{-2}\ \text{s}^{-1}) \tag{4}$$

where K_L is the mass transfer coefficient, C_s is the saturation concentration of the gas, and C is the bulk aqueous-phase concentration. Henry's law is used to calculate the saturation concentration of the dissolved gas at the gas/water interface

$$C_s = HP_i \quad (\text{mol m}^{-3}) \tag{5}$$

where H is Henry's constant and P_i is the partial pressure of the gas at that depth. Combining equations 4 and 5 yields

$$J_i = K_L (HP_i - C) \quad (\text{mol m}^{-2}\ \text{s}^{-1}) \tag{6}$$

Including the surface area of a bubble gives the rate of mass transfer for a single bubble of radius r

$$\frac{dm_i}{dt} = -K_L (HP_i - C) \cdot 4\pi r^2 \quad (\text{mol s}^{-1}) \tag{7}$$

The vertical location of the bubble is related to the bubble rise velocity, v_b, and any induced vertical water velocity, v, by

$$\frac{dz}{dt} = v + v_b \quad (m\ s^{-1}) \tag{8}$$

Assuming that any induced water velocity is negligible, combining equations 7 and 8 gives the mass transferred from a single bubble per unit height of tank

$$\frac{dm}{dz} = -K_L\left(HP_i - C\right)\cdot\frac{4\pi r^2}{v_b} \quad (mol\ m^{-1}) \tag{9}$$

Equation 9 is the discrete bubble model. The model is then modified to include the number of bubbles per second, N, or bubble number flux, which can be calculated from the initial bubble volume, V_o, and the gas flow rate at the diffuser, Q_z, or

$$N = \frac{Q_Z}{V_O} \quad (s^{-1}) \tag{10}$$

Multiplying equation 9 by N and expressing in terms of M_G, the molar flow rate of undissolved gas, yields

$$\frac{dM_G}{dz} = -K_L\left(HP_i - C\right)\cdot\frac{4\pi r^2 N}{v_b} \quad (mol\ m^{-1}\ s^{-1}) \tag{11}$$

Assuming that C does not change significantly during the time it takes for a bubble to rise to the surface of the tank, the pseudo-steady state assumption may be invoked. Equation 11 is integrated to obtain the change in molar flow rate of undissolved gas during the period the gas bubbles are in contact with the water in the tank. This value can then be used together with the usual well-mixed "batch reactor" equation to obtain the evolving aqueous concentration as a function of time. Note that in equation 11, H is a function of water temperature only, while v_b, and K_L are functions of r, the radius of the bubble. The bubble radius changes in response to decreasing hydrostatic pressure as well as a mass balance on the amount of oxygen and nitrogen transferred between the bubble and the water. Relationships for v_b, and K_L were developed by Wüest et al. (1992), based on the experimental measurements of bubble rise velocity (Figure 2) by Haberman and Morton (1956) and mass transfer coefficient (Figure 3) by Motarjemi and Jameson (1978) as summarized in Table 1.

Solution Procedure

The initial dissolved oxygen and nitrogen concentrations, temperature and water depth are known, as well as the initial bubble diameter formed at the diffuser. The initial conditions must be obtained to begin the iterative solution of equation 11. H is assumed constant while K_{OL} and v_b vary as a function of bubble radius, and are recalculated after every step. The initial mass flow rate of gaseous oxygen and nitrogen is given by

$$M_{Gi} = \frac{P_{std} Q_{std}}{RT_{std}} f_i \quad (\text{mol s}^{-1}) \tag{12}$$

where P_{atm} is atmospheric pressure, Q_{std} is the gas flow rate at standard temperature and pressure, f_i is the mole fraction of the gas, R is the ideal gas constant, and T_{std} is standard temperature.

The number flux of bubbles is defined by equation 10 and remains constant through the rise height, and time of the simulation. Equation 11 is then solved for the first step using the initial conditions. After the step, the new dissolved concentration, C, and the new mass flow rate of gas are calculated

$$M_{Gi} = M_{Gi-1} + \Delta M_{Gi} \quad (\text{mol s}^{-1}) \tag{13}$$

Next, the mole fraction is recalculated as

$$f_i = \frac{M_{Gi}}{\sum M_G} \tag{14}$$

where ΣM_G is the sum of molar flow rates of all of the gaseous species. The gas flow is then computed as

$$Q_{gas} = \frac{\Sigma M_G RT}{P_Z} \quad (\text{m}^3 \text{ s}^{-1}) \tag{15}$$

where P_Z is the pressure at the corresponding depth in the tank that the iteration is being calculated. The new bubble volume is

$$V = \frac{Q_{gas}}{N} \quad (\text{m}^3) \tag{16}$$

Next, the adjusted rise velocity and mass transfer coefficients are calculated from Table 1. A new calculation is then started using the new bubble condition. This procedure is continued until the top of the tank is reached. The entire procedure starts over with the next time step and with the new concentration until the desired dissolved oxygen concentration is obtained.

Results

The Sauter-mean diameter for the model input was estimated assuming a linear relationship for the Sauter-mean diameter formed at the diffuser as a function of gas flow rate (Figure 4). The correlation coefficient of the regression line, R^2, was 0.82 (Figure 4). The correlation equation for the initial bubble size is

$$d = \frac{0.237 Q_{std}}{L_d} + 1.12 \quad \text{(mm)} \tag{17}$$

where d is the Sauter-mean diameter, and L_d is the length of the soaker hose on the diffuser system, in this case 3 meters. To compare the model predictions with the mass transfer data, the average of the three multiprobe dissolved oxygen curves was employed (Figure 5). The measured and predicted dissolved oxygen curves were then compared with good results, with root mean square (RMS) errors below 0.51 in all cases (Figure 6). The curves diverge slightly in the range of 7 mg/L dissolved oxygen, and reconverge towards saturation levels. There are several possible reasons for these small discrepancies, which are discussed below. Overall, the results indicate that the Sauter-mean diameter leads to an accurate representation of the bubble size distribution and that the discrete bubble model when applied to a hypolimnetic oxygenation system will accurately describe the mass transfer.

Discussion

The model as described predicts the mass transfer data using fundamental principals with good accuracy. However, there are several factors that should be considered as causes for the slight deviations in the model predictions. Experimental errors could account for some of these discrepancies, including the effect of water depth fluctuations on initial bubble size, surface reaeration and measurement errors.

Figure 4 compares the Sauter-mean diameter of bubbles measured at a depth of 7 and 12.5 meters as a function of the volumetric air flow rate evaluated at the diffuser. While it can not be concluded that there is no relationship between bubble volume and depth to the diffuser, Figure 4 suggests that it is reasonable to assume that slight water level fluctuations have no effect on the initial bubble volume.

Because the mass transfer tests were conducted over a considerable amount of time, and the concentration driving force is high, some surface reaeration did occur. Surface reaeration resulting in increased oxygen transfer may have partially lead to the higher measured dissolved oxygen curve in Figure 6. However, this increase is not expected to be significant as the surface area to volume ratio of the tank is relatively small at 0.023 m^{-1}, and little turbulence is induced at the surface of the tank.

Additional error may be introduced through the initial bubble size measurements. The assumption that a linear relationship exists between the initial bubble size formed at the diffuser and the air flow rate may not be valid, which may result in a slight error in estimates of the initial bubble size used in the model. There was also a considerable amount of variance in the measured bubble sizes.

<u>Bubble Rise Velocity</u>

The model currently uses correlation equations developed by Wüest et al. (1992) for terminal bubble rise velocity as a function of bubble radius. The equations are based on

data collected by previous researchers (Haberman and Morton, 1956). In the range of 0.5 – 1 mm bubble radius, there is some discrepancy in the rise velocity data between bubbles rising in distilled water and tap water, with the Wüest et al. correlation falling in the middle of the two. In most environments where hypolimnetic oxygenation is used, the water will more closely resemble the tap water used in the experiments conducted by Haberman and Morton (1956). Because the bubbles in this range behave as a rigid sphere, the terminal rise velocity can be determined using Stoke's terminal velocity equation (Figure 2). Therefore, it is more appropriate to use Stoke's Law to calculate the terminal rise velocity for bubbles with a radius of 1 mm or less. An additional benefit of implementing Stoke's Law in this range of bubble sizes is the inclusion of temperature effects on bubble rise velocity. While not substantial, there is a slight change in bubble rise velocity as a function of temperature that could effect the predicted performance of a hypolimnetic oxygenation system.

If the bubble radius exceeds 1 mm, the bubble begins to become more fluid, and is less influence by surface particles (Motarjemi and Jameson, 1978). The bubble rise velocity remains fairly constant to a bubble radius of 5 mm, at which point it begins to increase again. Jamialahmadi et al. (1994) propose a correlation describing the terminal rise velocity over a wide range of bubble sizes based on Stoke's Law combined with a surface wave analogy. This correlation is reported to better represent the mechanics of bubble motion (Jamialahmadi et al., 1994).

Mass Transfer Coefficient

The mass transfer coefficient for a single bubble is estimated using a correlation equation developed by Wüest et al. (1992). This correlation calculates the mass transfer coefficient for oxygen and nitrogen as a function of bubble diameter for bubbles of a diameter less than approximately 1.3 mm, and assumes a constant mass transfer coefficient for bubbles larger than 1.3 mm in diameter (Figure 3). The data in Figure 3 were collected by Motarjemi and Jameson (1978) in a quiescent fluid, and the effects of temperature on the mass transfer coefficient were not investigated. Research suggests that a high water velocity past a bubble may increase the mass transfer coefficient (Jun and Jain, 1993). While this will not significantly impact a bubble-plume oxygen system, where induced water velocities are low, it may increase the mass transfer in the Speece Cone and full-lift hypolimnetic aerator, where the induced water velocities can exceed 1.0 m/s (McGinnis and Little, 1998; Burris and Little, 1998).

Bubble Size Distribution

The discrete-bubble model can account for a specified bubble size distribution by replacing N, the number of bubbles per second with an array and specifying N_i for each size class (Wüest et al., 1992), however, using the Sauter-mean diameter simplifies the calculation procedure. Slight discrepancies will occur as the Sauter-mean diameter may not accurately represent for the average bubble rise velocity or mass transfer coefficient in the bubble swarm. Small bubbles have decreasing rise velocities and mass transfer coefficients, which are both dependent on bubble diameter. To investigate the effect of

using the Sauter-mean diameter instead of the bubble size distribution, the discrete-bubble model was modified to account for an arbitrary bubble size distribution using three bubble size classes (Figure 7). The resulting dissolved oxygen curve was predicted using the Sauter-mean diameter of the bubble distribution and compared with the dissolved oxygen curve resulting from actual bubble size distribution for the same gas flow rate (Figure 7). Using the bubble size distribution results in slightly less oxygen transfer per unit time, which lowers the dissolved oxygen curve and results in a RMS difference of 0.28. This is similar to the difference seen between the measured and predicted oxygen transfer curves in Figure 6.

Induced Water Velocity

Another important assumption made during the testing of the model is that no vertical water velocity exists. In reality, an induced water velocity does exist, however, it was determined to be less than 0.04 m/s, the lower measurement limit of the velocity meter used. To test the effect of induced vertical water velocities, which decreases the bubble contact time, the discrete-bubble model was modified to include a uniform vertical velocity (Figure 8). For the conditions shown in Figure 8, there appears to be a minor decrease of 4% in oxygen transfer efficiency between 0 and 0.04 m/s. Because it is assumed that some vertical water velocity does exist, the resulting predicted dissolve oxygen profile would be slightly affected.

Conclusion

The discrete bubble model was presented, and verified using data collected in a 14-meter tank with good results. The model is applied to a diffused gas system by measuring the bubble size formed at the diffuser, and accounting for the number of bubbles produced at the diffuser per unit time. With relatively simple modifications, the model can also account for a range of bubble sizes formed at the diffuser; however, use of the Sauter-mean diameter is a reasonable and simpler approach. The model accounts for the effects of vertical water velocity on bubble contact time, however, the effects of high water velocities on the mass transfer coefficient are not known.

The discrete-bubble model has been applied to the full-lift hypolimnetic oxygenator with good success (Burris et al., 1999). The discrete-bubble model has also been applied to the Speece Cone; however, it has not been verified due to the unavailability of data (McGinnis and Little, 1998). Current work is underway to couple the discrete-bubble model with a hydrodynamic model for a linear bubble-plume diffuser. This suite of models for the Speece Cone, full-lift hypolimnetic oxygenator, and the bubble-plume diffuser will then be coupled with a reservoir and a cost model to optimize their design, and predict their performance and long term effects on the water body.

Acknowledgements

The National Science Foundation, Roanoke County, Virginia, and Tennessee Valley Authority provided financial support for this research. Special thanks are extended to Vickie Burris for her assistance in the field.

Nomenclature

A	surface area (m^2)
C	dissolved concentration (mol m^{-3})
d	bubble diameter (m) (mm)
f	mole fraction of gas (-)
H	solubility constant (mol m^{-3} bar^{-1})
J	mass transfer flux through single bubble surface (mol m^{-2} s^{-1})
K_{OL}	overall mass transfer coefficient (mol s^{-1})
L	diffuser length (m)
m	mass of gas (mol)
M	mass flux (mol s^{-1})
N	number flux of bubbles (s^{-1})
P	pressure (bar)
Q	volumetric flow rate (m^3 s^{-1})
r	bubble radius (m)
R	ideal gas constant (m^3 Pa K^{-1} mol^{-1})
t	time (s)
T	temperature (^oC) (K)
v	velocity (m/s)
V	volume (m^3)
z	depth (m)

Greek Letters

Δ	incremental change

Subscripts

3,2	Sauter-mean
atm	atmospheric
b	bubble
d	diffuser
G	gaseous
i	molar species
o	initial
s	saturation
std	standard temperature and pressure

References

Ashley, K. I., D. S. Mavinic, and K. J. Hall, Effects of orifice size and surface conditions on oxygen transfer in a bench scale diffused aeration system, *Envir. Tech.*, *11*, 609-618, 1990.

Ashley, K. I., K. J. Hall, and D. S. Mavinic, Factors influencing oxygen transfer in fine pore diffused aeration, *Wat. Res.*, *25*, 1479-1486, 1991.

Burris, V. L., J. C. Little, Oxygen transfer in a hypolimnetic aerator, *Water Sci. Technol.,* 37, 2, 1998.

Chen, S., M. B. Timmons, D. J. Aneshansley, and J. J. Bisogni, Jr., Bubble size distribution in a bubble column applied to aquaculture systems, *Aquaculture Eng.*, *11*, 267-280, 1993.

Cole, G. A., *Textbook of Limnology*, 4th ed., 412 pp., Waveland Press, Inc., Prospect Heights, IL, 1994.

Cooke, G. D. and R. E. Carlson, *Reservoir Management for Water Quality and THM Precursor Control*, 387 pp., AWWA Research Foundation, Denver, CO, 1989.

Haberman, W. L. and R. K. Morton, An experimental study of bubbles moving in liquids, *Proc. Am. Soc. Civ. Eng., 80,* 379-427, 1954.

Jamialahmadi, M., C. Branch and J. Müller-Steinhagen, Terminal rise velocity in liquids, *Trans IchemE*, 72, Part A, 1994.

Jun, K. S. and S. C. Jain, Oxygen transfer in bubbly turbulent shear flow, *J. Hyd. Eng., 119,* (1), 21-36, 1993.

Little, J. C., Hypolimnetic aerators: Predicting oxygen transfer and hydrodynamics, *Wat. Res*., *29*, 2475-2482, 1995.

McGinnis, D. F. and J. C. Little, Bubble dynamics and oxygen transfer in a Speece Cone. *Wat. Sci. Tech.*, *37,* (2), 285-292, 1998.

Mobley, M. H., TVA Reservoir Aeration Diffuser System, TVA Technical Paper 97-3, *ASCE Waterpower '97*, Atlanta, GA, August 5-8, 1997.

Motarjemi, M. and G. J. Jameson, Mass transfer from very small bubbles - The optimum bubble size for aeration, *Chemical Engineering Science, 33,* 1415-1423, 1978.

Orsat, V., Vigneault, C. and G. S. V Raghavan, Air Diffusers Characterization Using a Digitized Image Analysis System. *Applied Engineering in Agriculture,* 9, 1, 115-121, 1993.

Stefan, H. G. and X. Fang, Dissolved oxygen model for regional lake analysis, *Ecological Modelling*, 71, 37-68, 1994.

Wüest, A., N. H. Brooks, and D. M. Imboden, Bubble plume modeling for lake restoration, *Wat. Resour. Res*., *28*, 3235-3250, 1992.

Table 1. Correlation equations for Henry's Law constant, mass transfer coefficient, and bubble rise velocity (Wüest et al., 1992)

Equation	**Range**
$K_O = 2.125 \times 10^{-5} - 5.021 \times 10^{-7}T + 5.77 \times 10^{-9}T^2$ (mol m^{-3} Pa^{-1}) $K_N = 1.042 \times 10^{-5} - 2.450 \times 10^{-7}T + 3.171 \times 10^{-9}T^2$ (mol m^{-3} Pa^{-1})	(T in Celsius)
$K_{OL} = 0.6r$ (m s^{-1})	$r < 6.67 \times 10^{-4}$ m
$K_{OL} = 4 \times 10^{-4}$ (m s^{-1})	$r \geq 6.67 \times 10^{-4}$ m
$v_b = 4474r^{1.357}$ (m s^{-1})	$r < 7 \times 10^{-4}$ m
$v_b = 0.23$ (m s^{-1})	$7 \times 10^{-4} \leq r < 5.1 \times 10^{-3}$ m
$v_b = 4.202r^{0.547}$ (m s^{-1})	$r \geq 5.1 \times 10^{-3}$ m

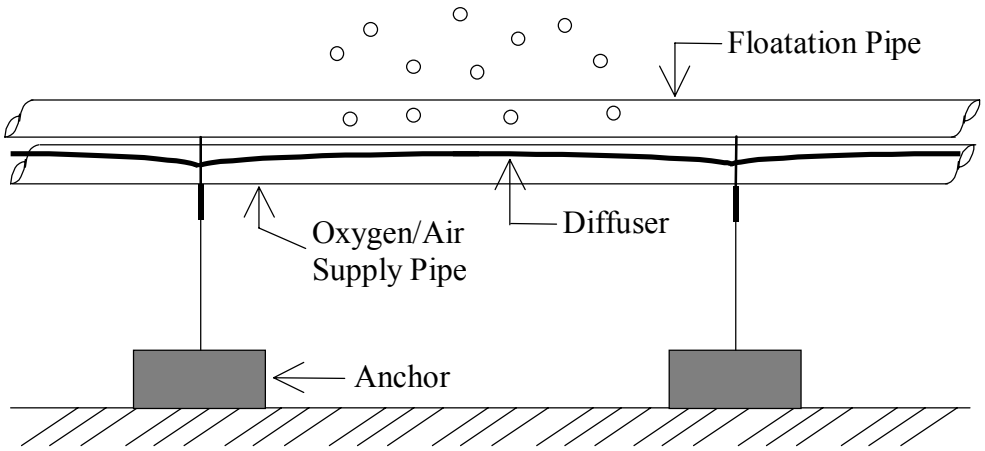

Figure 1. Schematic of TVA's soaker hose diffuser.

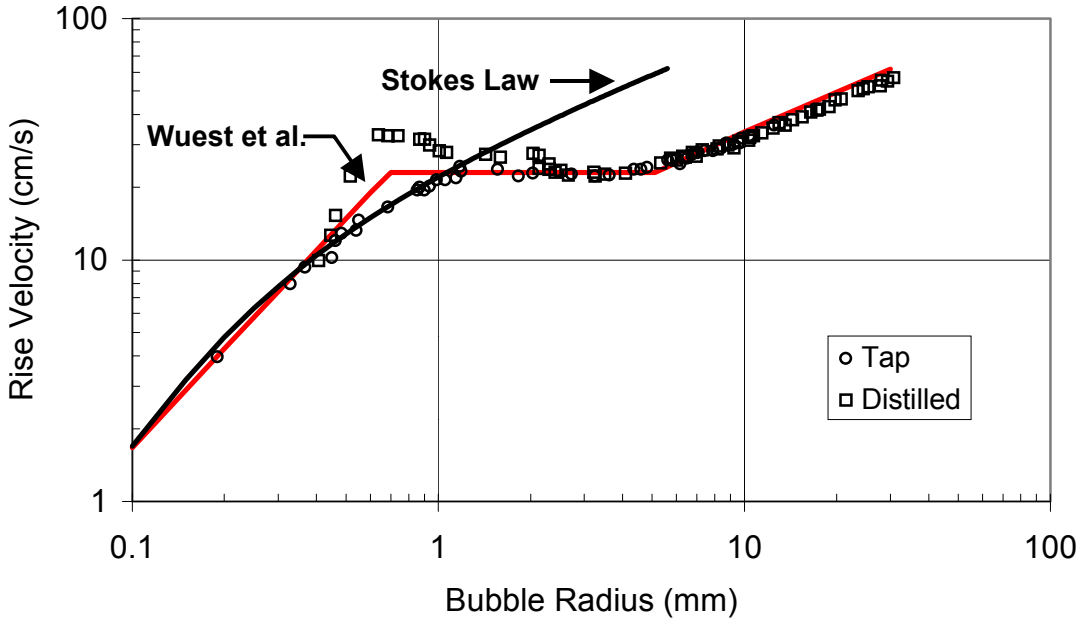

Figure 2. Terminal bubble rise velocity as a function of bubble radius. Data from Haberman and Morton, 1956.

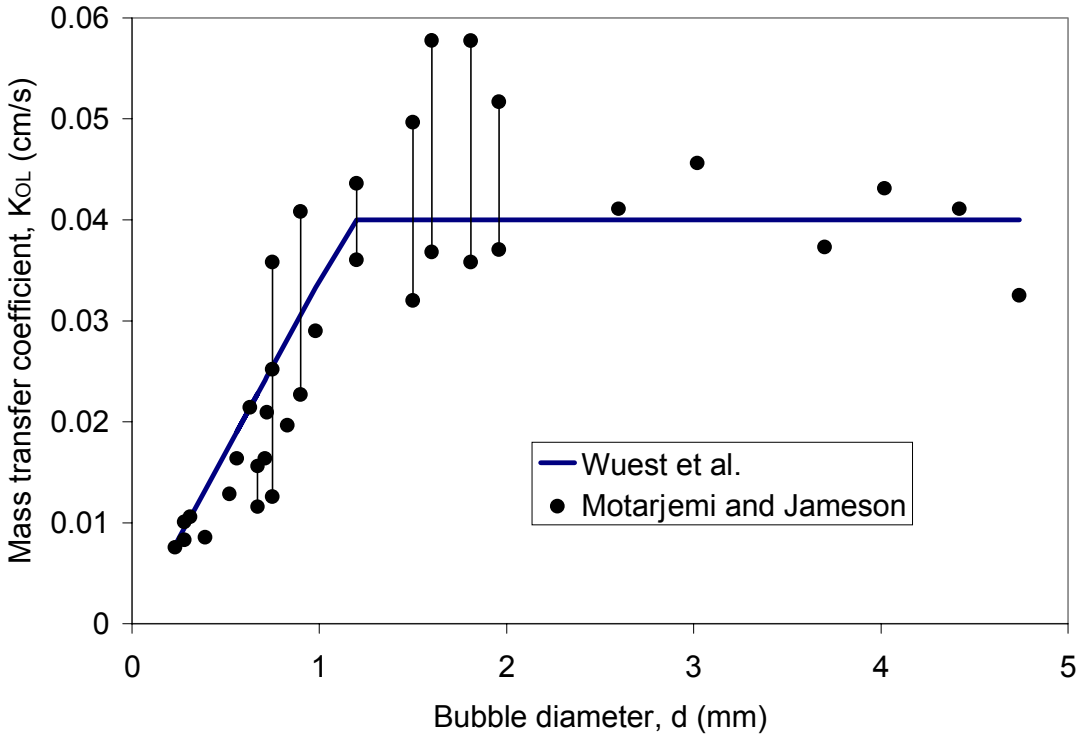

Figure 3. Mass transfer coefficient for a single bubble as a function of bubble diameter. Data from Motarjemi and Jameson, 1978.

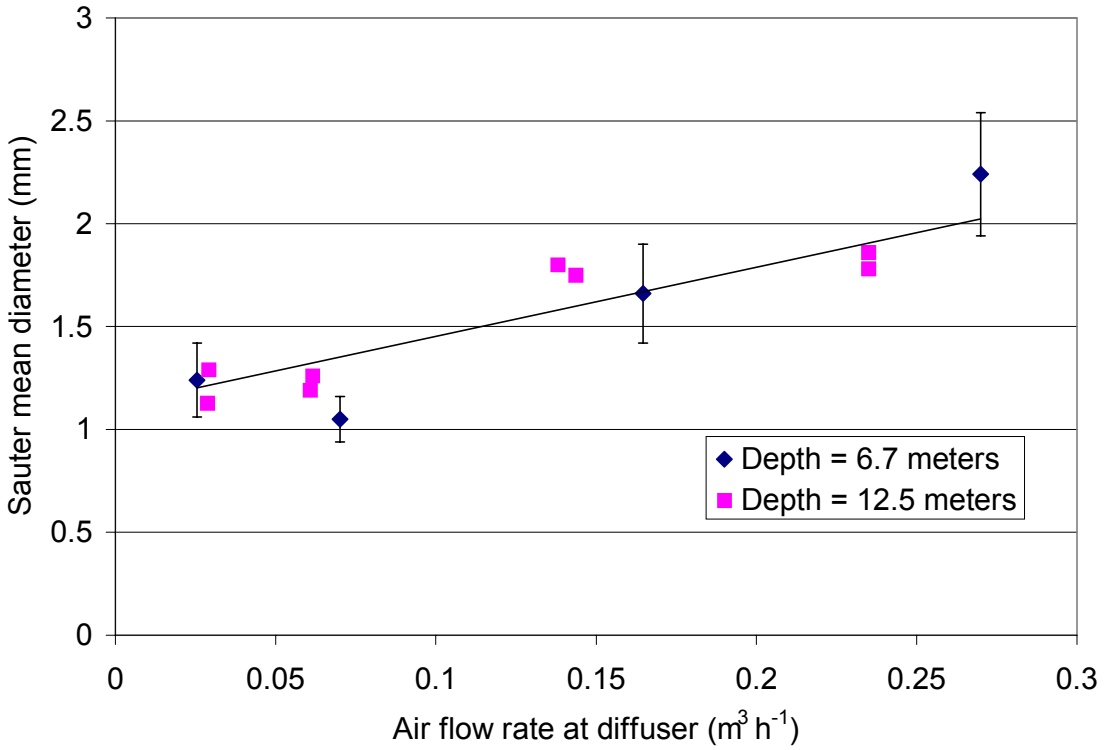

Figure 4. Comparison of initial bubble size formed at the diffuser for two depths with 95% confidence interval.

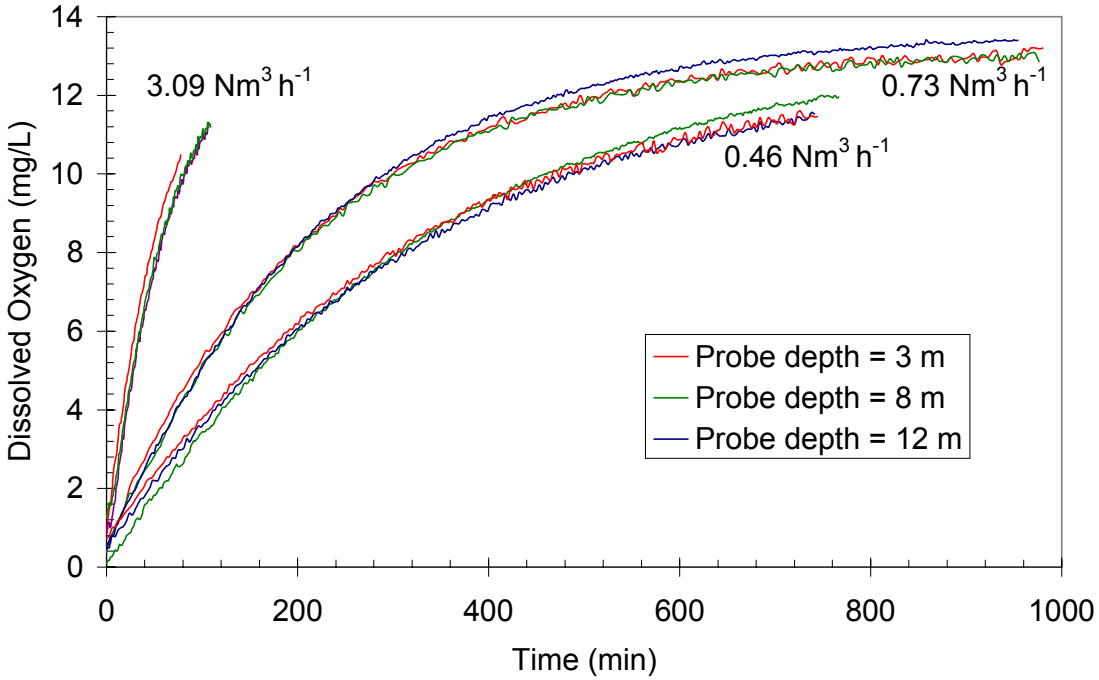

Figure 5. Mass transfer tests. Three dissolved oxygen probes indicating well-mixed conditions for each test.

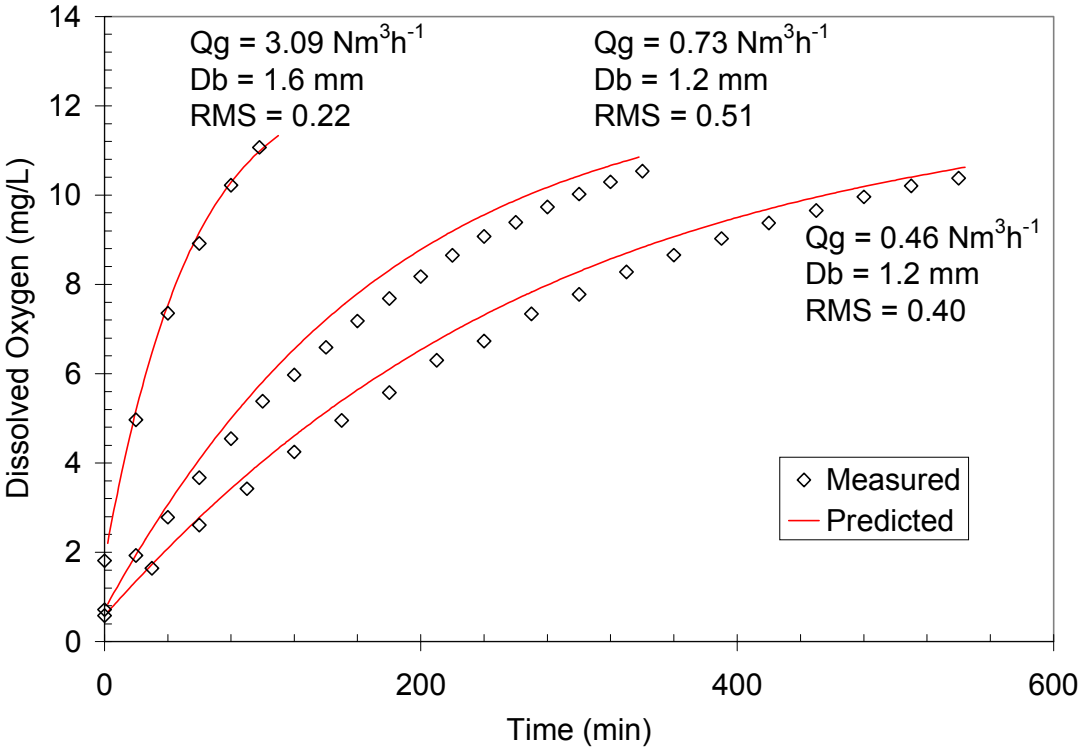

Figure 6. Discrete-bubble model predictions.

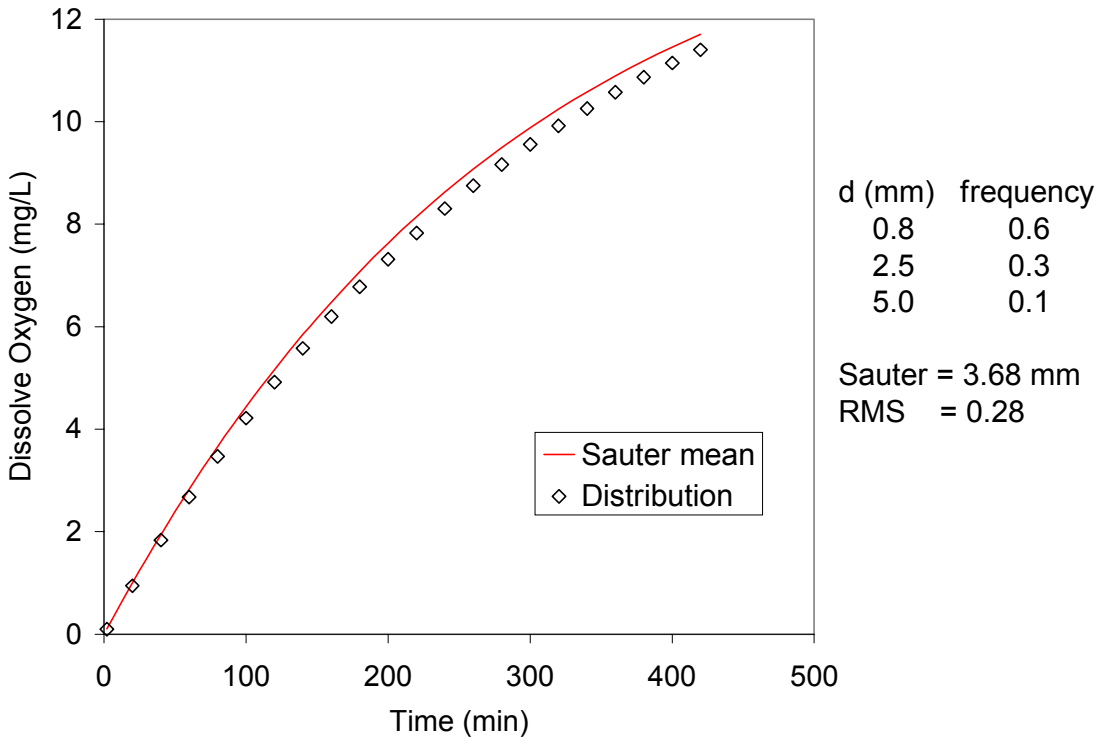

Figure 7. Comparison of effects of using bubble size distribution and the Sauter-mean diameter in the discrete-bubble model for an air flow rate of 0.73 $Nm^3\ h^{-1}$.

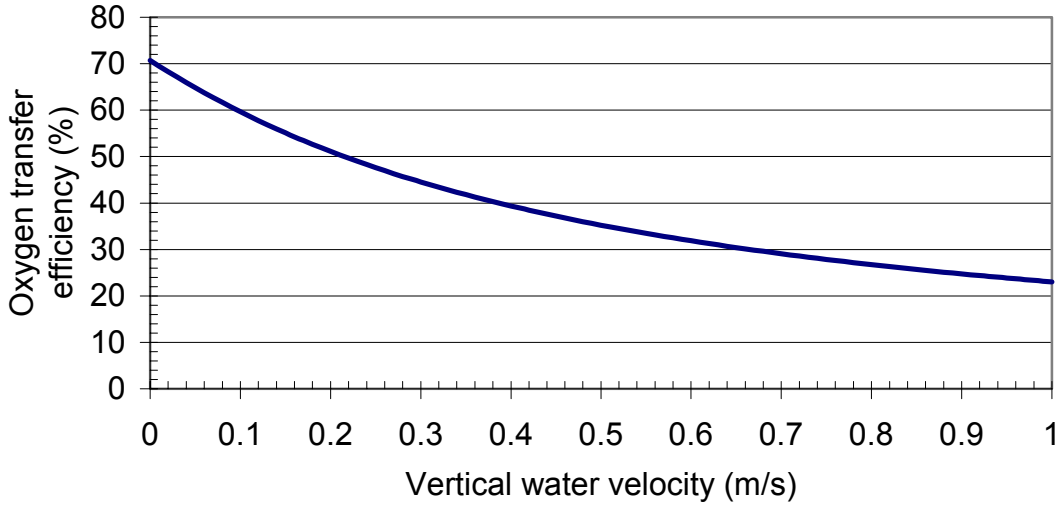

Figure 8. Effect of imposed vertical water velocity on oxygen transfer. The depth used in the simulation was 10 m, and an initial bubble diameter of 2 mm.

Wat. Sci. Tech. Vol. 37, No. 2, pp. 285-292, 1998.

CHAPTER 3. BUBBLE DYNAMICS AND OXYGEN TRANSFER IN A SPEECE CONE

Daniel F. McGinnis and John C. Little

Department of Civil Engineering, Virginia Polytechnic Institute and State University, Blacksburg, Virginia 24061-0105, USA

Abstract

A model is developed that predicts bubble dynamics and oxygen transfer in a Speece Cone. The model is based on differential mass balances for both gas and water and requires a knowledge of cone dimensions, water flow rate, depth to the cone, and initial bubble diameter produced by the oxygen diffuser. The model calculates the oxygen transfer, nitrogen stripping, and gas-phase holdup within the cone. Experimental data for a Speece Cone have not been published; however, a modified version of the model is tested using data obtained from a hydrodynamically similar full-lift hypolimnetic aerator with good results. This process model, when coupled with a suitable cost model, should prove useful in the preliminary design and economic optimization of Speece Cone oxygenator. © 1998 IAWQ. Published by Elsevier Science Ltd

Keywords

Aeration; gas holdup; hypolimnion; lake; model; oxygen transfer; reservoir; Speece Cone; water velocity.

Introduction

Depletion of oxygen in the hypolimnia of lakes and reservoirs can result in several undesirable changes in water quality including accelerated internal recycling of nutrients, solubilization of metals, and taste and odor problems that are undesirable in water supplies (Cooke et al., 1993). Of the various devices that are increasingly being used to replenish oxygen, full- and partial-lift hypolimnetic aerators, bubble-plume diffusers, and the Speece Cone are most common (McGinnis et al., 1997).

In this paper, a model that predicts gas-bubble dynamics and oxygen transfer in a Speece Cone is developed. The Speece Cone was invented by Dr. Richard Speece, who originally termed it a downflow bubble contactor (Speece et al., 1973; Thomas et al., 1994; Sanders, 1994). As shown in Figure 1, the device generally consists of a source of oxygen gas, a conical downflow bubble contact chamber, a submersible pump, and a

diffuser that disperses oxygenated water into the hypolimnion. Water and oxygen gas bubbles are introduced simultaneously at the top of the cone. The downward velocity of the water must be sufficient to overcome the rise velocity of the bubbles. The applied water flow rate and slope of the cone control the water velocity and hence the time available for gas transfer to occur. Because there is little hydraulic head loss, it is possible to economically pump a large volume of water through the cone (Speece et al., 1973). The model predicts oxygen transfer efficiency as a function of initial bubble size, gas and water flow rates, depth of operation, and the dimensions of the cone. Although experimental data for a Speece Cone have not yet been published, data from a hydrodynamically similar full-lift hypolimnetic aerator are available and have been used to validate the oxygen transfer model (Burris and Little, 1997). The performance of a Speece Cone over a range of operating conditions is examined using the model.

Model Development

The model is based on the known functional dependence of the bubble rise velocity and mass transfer coefficient on bubble size. It is assumed that the bubbles are spherical and of uniform initial size, that no bubble coalescence or breakup occurs, and that both water and gas are in plug flow. Mass balances for water and gas lead to a system of equations that incorporate gas transfer between the phases, the change in gas partial pressure with depth, the influence of gas holdup, and the changing radius of the cone. Figure 2 shows the basic dimensions of the Speece Cone. The radius, R, cross-sectional area, A, and superficial water velocity, v_s, vary with depth with

$$R = \frac{R_2 - R_1}{h} z + R_1 \quad (m)$$

$$A = \pi \left(\frac{R_2 - R_1}{h} z + R_1 \right)^2 \quad (m^2)$$

$$v_s = \frac{Q_w}{\pi} \left(\frac{R_2 - R_1}{h} z + R_1 \right)^{-2} \quad (m/s)$$

where Q_w is the water flow rate and z is the vertical coordinate defined as positive downwards.

Now, considering a single bubble within the cone, the mass transfer flux, J, across the surface is

$$J = K_{OL}(C_S - C) \quad (mol\ m^{-2}\ s^{-1})$$

where K_{OL} is the mass transfer coefficient, C_S is the saturation concentration of the gas, and C is the bulk aqueous concentration. An empirical correlation is used for both the

oxygen and nitrogen mass transfer coefficients as a function of bubble radius, as shown in Table 1. Henry's law is used to calculate the saturation concentration of the dissolved gas at the gas/water interface

$$C_S = KP_i \quad (\text{mol m}^{-3})$$

where K is Henry's constant and P_i is the partial pressure of the gas at a specific depth. Henry's constants are provided as empirical correlations in Table 1. Substituting Henry's law into the previous equation yields

$$J = K_{OL}\left(KP_i - C\right) \quad (\text{mol m}^{-2}\ \text{s}^{-1})$$

The velocity of the bubble relative to the cone walls is

$$\frac{dz}{dt} = v + v_b \quad (\text{m s}^{-1})$$

where v is the actual water velocity and v_b is the bubble rise velocity. Correlation equations for bubble rise velocity as a function of bubble radius are shown in Table 1. The actual water velocity is related to the superficial water velocity by

$$v = \frac{v_s}{1-\varepsilon_g} \quad (\text{m s}^{-1})$$

where ε_g is the gas holdup (total gas volume per unit volume of gas and water). This dimensionless quantity may be calculated using the ideal gas law

$$\varepsilon_g = \frac{\Sigma c_i RT}{P}$$

where Σc_i is the sum of the molar concentration of all gaseous species present. The initial gas holdup at the inlet of the cone is given (Wüest et al., 1992) by

$$\varepsilon_g = \frac{Q_{gas}}{\pi R^2\left(v + v_b\right)}$$

where Q_{gas} is the gas flow rate at the cone inlet. Assuming plug flow of gas bubbles, a mass balance yields the following transient equation

$$\frac{\partial c}{\partial t}A = -\left(\frac{\partial m}{\partial z}\right) - \frac{JNA_s}{v + v_b} \quad (\text{mol m}^{-1}\ \text{s}^{-1})$$

where m is the molar flow rate of the gas. N is the number of bubbles per unit time (calculated as Q_{gas}/V_o, where V_o is the initial bubble volume formed at the gas diffuser) and A_s is the surface area of a single bubble. Assuming steady state, and substituting for the flux and the surface area of a single bubble, the equation for the change in the molar flow rate of undissolved gas becomes

$$\frac{dm}{dz} = -K_{OL}\left(KP_i - C\right)\frac{4\pi r^2 N}{\left(v + v_b\right)} \quad (\text{mol m}^{-1}\ \text{s}^{-1})$$

where r is the radius of the bubble and m is defined as

$$m = \pi R^2 (v + v_b)c \quad (\text{mol s}^{-1})$$

By a similar analysis, the equation for the change in the molar flow rate of dissolved gas is

$$\frac{dM}{dz} = K_{OL}\left(KP_i - C\right)\frac{4\pi r^2 N}{\left(v + v_b\right)\left(1 - \varepsilon_g\right)} \quad (\text{mol m}^{-1}\ \text{s}^{-1})$$

where the molar flow rate of dissolved gas, M, is defined as

$$M = \pi R^2 vC \quad (\text{mol s}^{-1})$$

The result is a set of equations that describe the change in the molar flow rates of gaseous oxygen and nitrogen as well as dissolved oxygen and nitrogen with depth.

Model Validation

The set of differential equations comprising the model are solved simultaneously using Euler's Method. The model can predict oxygen transfer efficiency and gas holdup as a function of initial bubble size, applied gas and water flow rates, depth of operation, and the dimensions of the cone. Although experimental data for a Speece Cone have not yet been published, data from a hydrodynamically similar full-lift hypolimnetic aerator were available and have been used to validate the oxygen transfer model (Burris and Little, 1997). Although further details are given in that paper, a brief summary is provided here.

In the hypolimnetic aerator studied, air (as opposed to pure oxygen) is released at a depth of about 10 meters within a riser tube. The resulting air/water mixture, being less dense than the surrounding water, rises due to the imparted buoyancy. As the aerated water rises, oxygen is transferred from the air to the water at a rate that is proportional to the local concentration driving force. On reaching the top of the riser, the majority of air bubbles separate from the water and pass into the atmosphere, while the oxygenated water returns to the hypolimnion in the downcomer. The riser tube thus resembles an inverted Speece Cone that is cylindrical rather than conical in shape. In the experimental study (Burris and Little, 1997), the dissolved oxygen concentration profile in the riser tube was measured, as well as the induced water flow rate and the overall gas holdup. This was done for a range of applied air flow rates. With respect to the oxygen transfer model, the only unknown is the initial bubble size. The model was tested by finding the initial bubble size that resulted in the closest fit of the predicted to the experimentally

measured oxygen concentration profiles. Good fits were obtained for the entire range of air flow rates with estimated initial bubble diameters varying between 2.3 and 3.1 mm. These values are similar to what might be expected for the installed coarse-bubble diffusers. Once the initial bubble size was found, the overall gas holdup was calculated with the model. The predicted holdups were within about 30% of the experimentally observed values, providing further evidence for the validity of the model (Burris and Little, 1997).

Results and Discussion

Although not tested against experimental data from a Speece Cone, the model appears sufficiently robust to proceed with some preliminary predictions of performance. The conditions listed in Table 2 were used as a basis for the performance evaluation.

The high water flow rate, coupled with the high oxygen transfer efficiency, allows the cone to transfer a total of approximately 12,800 kg-O_2/day. The water is predicted to exit the cone with a dissolved oxygen concentration of 103 mg/L, although this is only 32% of the theoretical saturation concentration of 318 mg/L. The high oxygen transfer capacity is due to the relatively long bubble contact time, calculated to be 62 seconds for the baseline conditions.

Table 3 shows the predicted performance of the Speece Cone at different depths. The baseline conditions listed in Table 2 are kept constant, although the standard gas flow rate is adjusted to provide the equivalent volumetric gas flow rate (20.5 L/s) at the cone inlet for each depth. The predicted oxygen transfer efficiencies are all within 92 - 93%. These calculations suggest that the Speece Cone is very flexible in its applications.

Calculations using the model reveal considerable sensitivity to initial bubble size. If the initial bubble diameter is large, the bubbles do not dissolve quickly enough, and accumulate within the cone. This causes the gas holdup to increase at that depth, with a severe impact on the assumption that no bubble coalescence occurs. Figure 3 shows the effect of increasing the initial bubble diameter on the gas holdup within the Speece Cone.

As shown in Figure 3, for a 2.5 mm diameter bubble, the gas holdup approaches 6%. This indicates that the bubbles are reaching a condition of temporary vertical stasis at a depth of about 4.5 m. It should be noted that the predicted gas holdup is also highly dependent on water flow rate and oxygen flow rate. If the water flow rate is increased, or the oxygen flow rate is decreased, the gas holdup will be lower for the bubble sizes shown.

The oxygen transfer model also accounts for the stripping of nitrogen gas by the bubbles. Figure 4 shows both the dissolved nitrogen and oxygen concentration profiles within the cone for the baseline conditions.

The most rapid increase in the oxygen concentration occurs in the middle region of the cone, where the bubble velocity relative to the cone is the slowest. Towards the outlet of the cone, the dissolved oxygen concentration drops off rather rapidly because the partial pressure of oxygen is decreasing as the partial pressure of nitrogen within the bubble increases. The dissolved nitrogen is stripped in the upper region of the cone, but, as the partial pressure of nitrogen within the gas bubble increases, the nitrogen begins to redissolve.

Conclusion

A model has been developed that predicts bubble dynamics and oxygen transfer within a Speece Cone. Although no published experimental data for a Speece Cone are available, the model was validated using data taken from an experimental study of a full-lift hypolimnetic aerator (Burris and Little, 1997). The model predictions are sensitive to the initial bubble diameter produced by the gas diffuser. If too large a bubble is produced, the performance of the cone may be compromised. The water and oxygen gas flow rates also have a substantial impact on the performance of the cone. This process model, when coupled with a suitable cost model, should prove useful in the preliminary design and economic optimization of Speece Cone oxygenators.

Nomenclature

A	area (m^2)
A_s	surface area of a bubble (m^3)
C	dissolved concentration (mol m^{-3})
C	gaseous concentration (mol m^{-3})
h	height (m)
J	mass transfer flux through single bubble surface (mol m^{-2} s^{-1})
K	Henry's constant (mol m^{-3} bar^{-1})
K_{OL}	overall mass transfer coefficient (mol s^{-1})
m	molar flow rate of undissolved gas (mol s^{-1})
M	molar flow rate of dissolved gas (mol s^{-1})
N	number flux of bubbles (s^{-1})
P	pressure (Pa)
Q	volumetric flow rate (m^3 s^{-1})
r	bubble radius (m)
R	ideal gas constant (m^3 Pa K^{-1} mol^{-1})
R	radius (m)
T	temperature (^oC) (K)
v	velocity (m/s)
z	depth (m)

Greek Letters

ε	gas hold up

Subscripts

b	bubble
i	represents gaseous species
g	gas
s	superficial, surface area
S	saturation

References

Burris, V. L., Little, J. C. (1997) Oxygen transfer in a hypolimnetic aerator. In Proceedings of the IAWQ/IWSA Joint Specialist Conference, Reservoir Management and Water Supply - an Integrated System, Prague, Czech Republic, 19-23 May, 1997.

Cooke, G. D, Welch, E. B., Peterson, S. A. and Newroth, P. R. (1993). *Restoration and Management of Lakes and Reservoirs*. 2nd edn, Lewis Publishers, Boca Raton.

McGinnis, D., Little, J. and Cumbie, W. (1997) Nutrient control in Standley Lake: Evaluation of three oxygen transfer devices. In Proceedings of the IAWQ/IWSA Joint Specialist Conference, Reservoir Management and Water Supply - an Integrated System, Prague, Czech Republic, 19-23 May, 1997.

Sanders, J. O. Jr. (1994) Camanche hypolimnetic oxygenation demonstration project. East Bay Municipal Utility District, Oakland, California.

Speece, R. E., Rayyan, F. and Murfee, G. (1973). Alternative considerations in the oxygenation of reservoir discharges and rivers. In: *Applications of commercial oxygen to water and wastewater systems*. R. E. Speece and J. F. Malina, Jr. (Ed.), Center for Research in Water Resources, Austin Texas, pp. 342 - 361.

Thomas, J. A., Funk, W. H., Moore, B. C. and Budd, W. W. (1994) Short term changes in Newman Lake following hypolimnetic aeration with the Speece Cone. *Lake and Reservoir Management*. 9, 1, 111 - 113. Extended Abstract of a paper presented at the 13th International Symposium of the North American Lake Management Society, Seattle, WA, Nov. 29 - Dec. 4, 1993.

Wüest, A., Brooks, N. H., and Imboden, D. M. (1992) Bubble plume modeling for lake restoration. *Water Resources Research,* 28, 12, 3235-3250.

Table 1. Correlation equations for Henry's Law constant, mass transfer coefficient, and bubble rise velocity (Wüest et al., 1992)

Equation	**Range**
$K_O = 2.125 \times 10^{-5} - 5.021 \times 10^{-7}T + 5.77 \times 10^{-9}T^2$ (mol m^{-3} Pa^{-1}) $K_N = 1.042 \times 10^{-5} - 2.450 \times 10^{-7}T + 3.171 \times 10^{-9}T^2$ (mol m^{-3} Pa^{-1})	(T in Celsius)
$K_{OL} = 0.6r$ (m s^{-1})	$r < 6.67 \times 10^{-4}$ m
$K_{OL} = 4 \times 10^{-4}$ (m s^{-1})	$r \geq 6.67 \times 10^{-4}$ m
$v_b = 4474r^{1.357}$ (m s^{-1})	$r < 7 \times 10^{-4}$ m
$v_b = 0.23$ (m s^{-1})	$7 \times 10^{-4} \leq r < 5.1 \times 10^{-3}$ m
$v_b = 4.202r^{0.547}$ (m s^{-1})	$r \geq 5.1 \times 10^{-3}$ m

Table 2. Baseline conditions and predicted performance

Cone Dimensions	
Inlet Radius (m)	0.3
Outlet Radius (m)	1.8
Height (m)	6
Operational Parameters	
Oxygen Concentration (mg/L)	2
Water Temperature (^{o}C)	10
Depth to Inlet (m)	50
Initial Bubble Diameter (mm)	2
Water Flow Rate (m^3/s)	1.5
Oxygen Flow Rate (L/s)	120
Performance	
Change in Dissolved Oxygen (mg/L)	101
Total Oxygen Added (kg-O_2/day)	12800
Oxygen Transfer Efficiency (%)	93
Bubble Residence Time (second)	62

Table 3. Speece Cone performance at varying depths

Depth (meters)	Q_{gas} (L/s)	ΔC_{O2} (mg/L)	Total Oxygen Transfer (kg-O_2/day)	Bubble Residence Time (seconds)
0	20.5	17	2200	107
10	40.4	33	4300	75
20	60.3	50	6400	69
30	80.2	66	8600	66
40	100.1	83	10700	64
50	120	101	12800	62

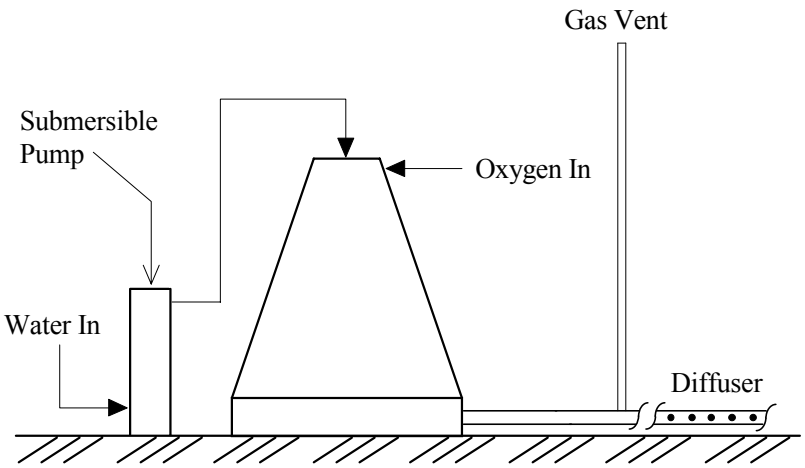

Figure 1. Diagram of a Speece Cone

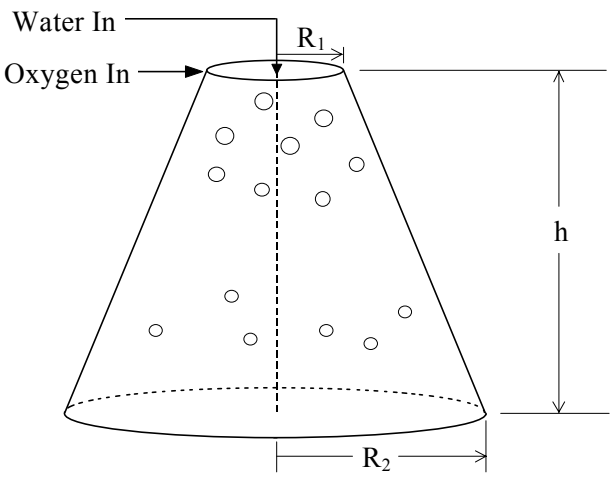

Figure 2. Speece Cone dimensions

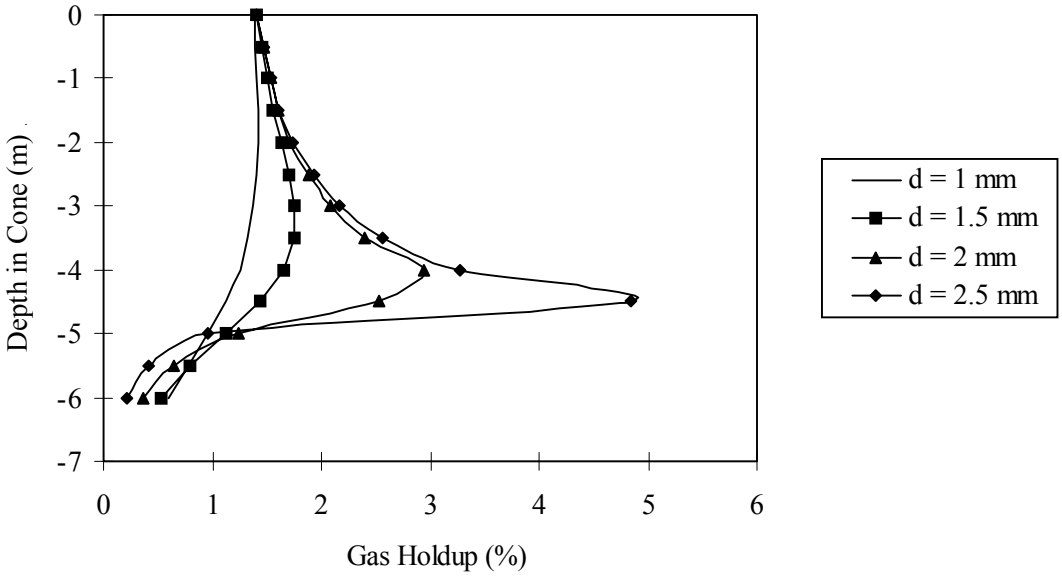

Figure 3. Effect of initial bubble diameter on gas holdup

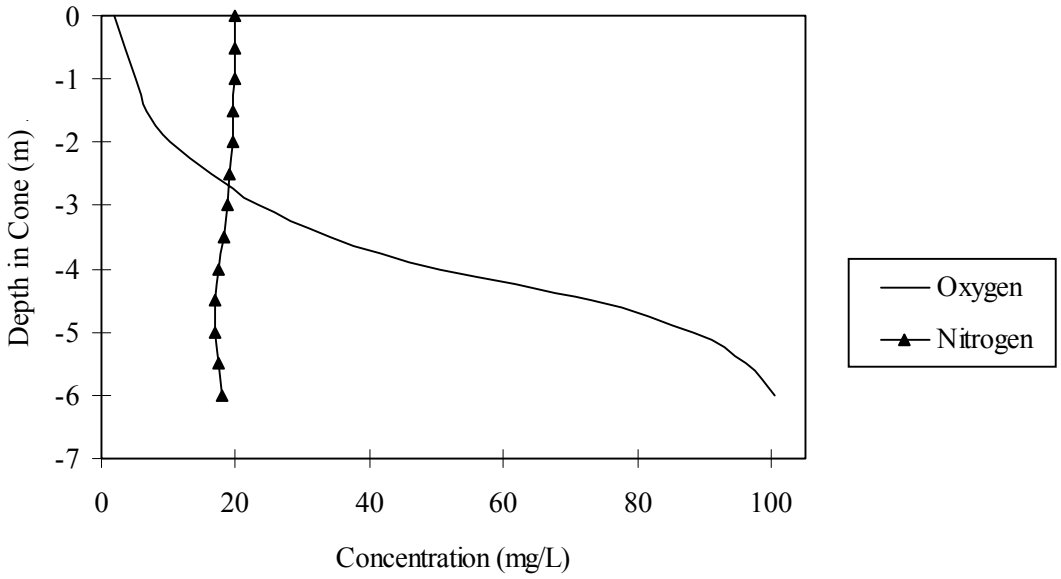

Figure 4. Dissolved oxygen and nitrogen profile within the Speece Cone

CHAPTER 4. HYPOLIMNETIC OXYGENATION: PREDICTING PERFORMANCE USING A DISCRETE-BUBBLE MODEL

D. F. McGinnis and J. C. Little

Department of Civil & Environmental Engineering, Virginia Polytechnic Institute and State University, Blacksburg, Virginia 24061-0246, USA

Abstract

Stratification of water-supply reservoirs frequently results in substantial hypolimnetic oxygen depletion with a resulting negative impact on raw water quality. Hypolimnetic oxygenators are used to add oxygen to the hypolimnion without significantly disrupting the thermal density structure. The three most common devices are the hypolimnetic aerator, the Speece Cone, and the bubble-plume diffuser. A discrete-bubble model based on fundamental principles has previously been shown to hold considerable promise for predicting the performance of full-lift hypolimnetic aerators and the Speece Cone. In this paper, we have further verified this model by comparing its predictions to a series of pilot-scale experimental measurements collected under controlled conditions and have also demonstrated its ability, under somewhat idealized conditions, to predict the full-scale performance of a bubble-plume diffuser in a stratified reservoir. The potential for the diffused-bubble aeration system to increase oxygen demand, and the rate at which nitrogen builds up during operation and de-gasses following destratification, are also briefly considered.

Keywords

Aeration; discrete-bubble model; hypolimnion; nitrogen, oxygen transfer; reservoir

Introduction

Thermal stratification of lakes and reservoirs frequently results in substantial hypolimnetic oxygen depletion (Cooke and Carlson, 1989). Low dissolved oxygen (DO) levels have a negative impact on cold-water fisheries, hydropower generation, and the drinking-water treatment process. In water-supply reservoirs, low DO may lead to the production of hydrogen sulfide and ammonia, and can cause the release of phosphorus as well as reduced iron and manganese from the sediments. Increased phosphorus concentrations may stimulate algal growth, which exacerbates the problem because dead algae ultimately fuel additional oxygen demand. Iron, manganese and hydrogen sulfide impart undesirable color, taste, and odor to the water requiring additional treatment prior to distribution (Cooke and Carlson, 1989). The increased chlorine demand at the water

treatment plant can be costly, and the additional chlorine may react with natural organic matter producing disinfection-by-products.

When applied in stratified reservoirs, well-designed hypolimnetic oxygenators have been shown to provide measurable increases in hypolimnetic dissolved oxygen levels (Gachter, 1995), decrease total iron, manganese, and hydrogen sulfide concentrations (McQueen and Lean, 1986; Thomas et al., 1994), and decrease blue-green algae concentrations in some cases (Kortmann et al., 1994; Gemza, 1995). There are three principle devices typically used for hypolimnetic oxygenation: the Speece Cone, the full- or partial-lift hypolimnetic aerator (Little, 1995), and, the focus of this paper, the bubble-plume diffuser (Wüest et al., 1992). In bubble-plumes, gas bubbles (either air or oxygen) are introduced into the water by means of diffusers and rise naturally through the water column upon release. In so doing, they entrain surrounding water, creating an unconfined, buoyant plume.

Although considerable research has been conducted on the hydraulic performance of bubble plumes (see, for example, Schladow, 1993) the first comprehensive model that included the effect of oxygen transfer was developed by Wüest et al. (1992). In that analysis, correlation equations were developed from previously published data relating bubble-rise velocity and the mass-transfer coefficient to bubble radius. The relationships were then used to predict oxygen transfer within the rising buoyant plume. This discrete-bubble approach has subsequently been shown to hold considerable promise for predicting the performance of full-lift hypolimnetic aerators (Burris and Little, 1998) and the Speece Cone (McGinnis and Little, 1998). In this paper, we will briefly review the development of the discrete-bubble model, validate it with pilot-scale experimental data, and then show how it may be applied, under somewhat idealized conditions, to predict the oxygenation capacity of a field-scale bubble-plume diffuser in a water-supply reservoir. Since dissolved nitrogen builds up in the hypolimnion during the aeration process, the time required for complete de-gassing of the nitrogen will be evaluated using a simple mass-transfer model.

Discrete-Bubble Model

Consider, as shown in Figure 1, discrete bubbles rising in plug flow through a well-mixed volume of water. The mass transfer flux, J, across the bubble surface is

$$J = K_L \left(HP_i - C \right) \quad [\text{mol m}^{-2}\ \text{s}^{-1}] \tag{1}$$

where K_L is the mass transfer coefficient, H is Henry's constant, P_i is the partial pressure of the gas at that depth, and C is the bulk aqueous concentration. A steady-state mass balance over a thin slice of the tank (see Figure 1) yields

$$\frac{dM_G}{dz} = -\frac{JNA_s}{v_b} \quad [\text{mol m}^{-1}\ \text{s}^{-1}] \tag{2}$$

where M_G is the molar flow rate of undissolved gas, and z is the vertical coordinate. N is the number of bubbles introduced per unit time calculated as Q_{gas}/V_o, where V_o is the initial volume of a single bubble formed at the diffuser. A_s is the surface area of a bubble and v_b is the bubble rise velocity. Substituting for the flux and the surface area of a bubble, equation 2 becomes

$$\frac{dM_G}{dz} = -K_L\left(HP_i - C\right)\frac{4\pi r^2 N}{v_b} \quad [\text{mol m}^{-1}\ \text{s}^{-1}] \tag{3}$$

where r is the radius of the bubble. If C does not change significantly during the time it takes for a bubble to rise to the surface of the tank, the pseudo-steady state assumption may be invoked. Equation 3 is integrated to obtain the change in the molar flow rate of undissolved gas during the period the gas bubbles are in contact with the water. This value can then be used to predict the evolving aqueous concentration in the well-mixed tank as a function of time. Note that in equation 3, K_L and v_b are functions of r, the bubble radius, and that r changes in response to decreasing hydrostatic pressure as well as a mass balance on the amount of oxygen and nitrogen transferred between the bubbles and the water. Correlations are used for the bubble-rise velocity and the mass transfer coefficient as a function of bubble radius (Wüest et al., 1992).

To validate the discrete-bubble model, mass-transfer experiments were conducted in a 14 m deep tank with a 1.5 m length of rubber porous-hose diffuser located at the bottom. The water was deoxygenated prior to the test using sodium sulfite, and the applied air flow rates were 0.46, 0.73, and 3.1 $Nm^3\ h^{-1}$, respectively (1 Nm^3 = 1 m^3 of gas at 1 bar and 0^{o}C). Data were collected using three DO probes at depths of 3, 8, and 12 m. The response of the three probes at each air flow rate was essentially identical, indicating that the water in the tank was relatively well-mixed during aeration. Data from the three probes were then averaged and plotted in Figure 2 as discrete symbols, for each of the three experimental air flow rates. Photographs were taken of the bubble swarm through a porthole located near the bottom of the tank. The resulting images were digitized and the bubble size distribution was measured using image analysis software. The results were used to estimate the Sauter-mean Diameter, $d_{3,2}$, created by the diffuser as a function of air flow rate, as defined by Orsat et al. (1993):

$$d_{3,2} = \frac{\sum_{i=1}^{n} d_i^3}{\sum_{i=1}^{n} d_i^2}$$

where d_i is the diameter of the individual bubbles. The appropriate value was then used as input to the discrete-bubble model and the evolving oxygen concentration in the tank was predicted for each of the three air flow rates, as shown in Figure 2. The good agreement between the observed and predicted data confirms that the discrete-bubble

model accurately represents mass-transfer taking place while the bubbles rise through the tank.

Bubble-Plume Diffuser

Table 1 provides details of a bubble-plume diffuser installed in Spring Hollow Reservoir and tested during Fall of 1998. The aeration system was started on September 28, and operated continuously through October 13 at which point it was switched off due to problems with a compressor. Temperature and DO profiles were measured prior to, during, and after this period of aeration to evaluate performance. The experimental profiles were taken at a point approximately 100 m away from one end of the diffuser. As shown in Figure 3, the hypolimnetic oxygen concentration at this sampling station increased from about 2 g m^{-3} prior to aeration to 6 g m^{-3} on October 9. The oxygen concentration presumably continued to increase through October 13, when the system was turned off. Unfortunately, sampling data were not collected at termination.

Figures 3 and 4 show that the temperature and oxygen concentration profiles in the hypolimnion became virtually uniform after aeration started. This suggests that the entire hypolimnetic volume above the diffuser was relatively well-mixed. In addition, a careful examination of Figure 4 reveals that some exchange took place between the hypolimnetic water volume (between 27 and 54 m) and the water in the lower thermocline (between 18 and 27 m).

Following shut-down, the hypolimnetic oxygen concentrations decreased, returning the hypolimnion to roughly its pre-aerated condition by October 28. Oxygen concentration profiles, together with information on reservoir volume, were used to estimate the hypolimnetic oxygen content prior to, during, and after aeration, as shown in Figure 5. Note that the well-mixed assumption is probably good during aeration, but may not be as reliable in the periods prior to and after aeration. On average, the analysis shows an oxygen consumption rate of 50 kg d^{-1} prior to aeration and an oxygen increase of 170 kg d^{-1} during aeration. Assuming the consumption rate of 50 kg d^{-1} remains constant during aeration, this translates into an overall oxygen addition rate of 220 kg d^{-1}. Since the diffuser was supplying oxygen at roughly 290 kg d^{-1} the system was operating at an efficiency of about 80%.

Upon closer examination, the data presented in Figure 5 suggest that the oxygen consumption rate may not have been constant during the entire period, as might have been expected. The rate of increase in oxygen content immediately after the aeration system was turned on appears to have been higher than the average rate of increase. In addition, the rate of decrease after aeration was turned off was also initially higher. A possible explanation is that mixing significantly increased the dissolved oxygen concentration gradient between the bulk water and the sediments (see Figure 3) and that this in turn may have increased the overall oxygen uptake rate by the sediments, assuming that the external oxygen transfer rate was limiting. If true, this may be a case

of what has sometimes been referred to in the literature as "aerator induced sediment oxygen demand."

Application of Discrete-Bubble Model to Bubble-Plume Diffuser

Since the hypolimnetic reservoir volume was essentially well-mixed while the diffuser was in operation, the conditions in the hypolimnion approximate those in the previously described tank experiment. The key difference is that while oxygen is being added by the diffuser, it is also being consumed by various processes in the hypolimnion. Assuming, as previously calculated, that the oxygen consumption rate was constant and equal to 50 kg d^{-1}, this quantity was incorporated in the discrete-bubble model analysis and used to predict the rate of increase in DO. The initial bubble-size had previously been determined as a function of air flow rate, and was therefore known for the specific diffuser operating conditions. The predicted hypolimnetic oxygen content, as shown in Figure 5, compares well to the measured values, although the model tends to over-predict the rate of oxygen transfer. There are at least two possible explanations for the modest discrepancy. Either the hypolimnetic oxygen consumption rate increased as a result of the induced mixing (as previously suggested), or the plume created by the diffuser transported the bubbles through the hypolimnion at a slightly faster rate than the predicted bubble-rise velocity (in other words, at a rate equal to the plume velocity plus the terminal rise velocity), providing less time for oxygen transfer than predicted by the model.

De-Gassing of Dissolved Nitrogen

While using air instead of pure oxygen may be more economical, one major concern is the build-up of dissolved nitrogen gas in the reservoir. This is of interest because of the potential for gas bubble disease in fish as well as the possible formation of nitrogen bubbles during the down-stream water treatment process. In December 1999, after the aeration system had been shut off, a total dissolved gas (TDG) probe was used to determine the dissolved nitrogen concentration. The TDG probe was anchored at a location close to the dam at a depth of 36 meters (see Figures 3 and 4) and used to continuously monitor TDG in addition to dissolved oxygen and water temperature. Measurements were made before, during and after stratification as shown in Figures 6 and 7. The results show that dissolved nitrogen levels reached about 180% saturation with respect to atmospheric pressure and ambient water temperature. Further examination of the data suggests that the final destratification process began on about December 23 and was largely completed by December 24, although some additional mixing occurred through December 26.

The time required for the dissolved nitrogen to de-gas from the reservoir was estimated using a simple mass transfer model. The surface mass-transfer coefficient K_L was determined assuming that the entire reservoir was more-or-less well mixed from December 24 onwards. The value for nitrogen was estimated as K_{Ln} = 1.9 m/d, with the exponential data fit shown in Figure 6. Neglecting any oxygen consumption in the reservoir, the mass transfer coefficient for oxygen was found to be K_{Lo} = 1.7 m/d, in good agreement with the value for nitrogen. These values are also in reasonable agreement with those predicted using the correlation equations given by Schwarzenbach et al. (1993) taking into account wind speed and water temperature. Using K_L for nitrogen, the time taken for the water in Spring Hollow Reservoir to reach a dissolved nitrogen level of 105% saturation (with respect to the atmosphere) was estimated to be 27 days, assuming similar wind speeds and that no significant re-stratification occurred.

Conclusions

The discrete-bubble model has previously been shown to hold considerable promise for predicting the performance of full-lift hypolimnetic aerators (Burris and Little, 1998) and the Speece Cone (McGinnis and Little, 1998). In this paper, we have further verified the model by comparing its predictions to a series of pilot-scale experimental measurements collected under controlled conditions, and have also demonstrated its ability, under somewhat idealized conditions, to predict the full-scale performance of a bubble-plume diffuser in a stratified water-supply reservoir. We have also shown that hypolimnetic mixing induced by the diffuser may be responsible for an increase in the sediment oxygen demand rate. However, this assessment was based on sampling at only one location within the reservoir, and a more thorough experimental analysis needs to be completed before firm conclusions can be drawn. It was also shown that the dissolved nitrogen that builds up during aeration takes roughly a month to de-gas following final destratification of the water column. Surface exchange mass transfer coefficient estimated from both nitrogen and oxygen data were in reasonable agreement with one another as well as with literature values.

Nomenclature

A_s	surface area of a bubble (m^3)
C	dissolved concentration (mol m^{-3})
J	mass transfer flux through single bubble surface (mol m^{-2} s^{-1})
K_L	overall mass transfer coefficient (mol s^{-1})
H	Henry's constant (mol m^{-3} bar^{-1})
M	molar flow rate of dissolved gas (mol s^{-1})
N	number flux of bubbles (s^{-1})
P	pressure (Pa)
Q	volumetric flow rate (m^3 s^{-1})
r	bubble radius (m)
v	velocity (m/s)

V volume (m^3)
z depth (m)

References

Burris, V. L. and Little, J. C. (1998). Bubble dynamics and oxygen transfer in a hypolimnetic aerator, *Water Science & Technology*, **37** (2) 293-300.

Cooke, G.D. and Carlson, R.E. (1989). *Reservoir Management for Water Quality and THM Precursor Control*. AWWA Research Foundation, Denver, CO.

Gachter, R. (1995). Ten years experience with artificial mixing and oxygenation of prealpine lakes. *Lake and Reserv. Manage.*, **11**, 141.

Gemza, A. (1995). Some practical aspects of whole lake mixing and hypolimnetic oxygenation. Ecological impacts of aeration on lakes and reservoirs in southern Ontario. *Lake and Reserv. Manage.*, **11**, 141.

Kortmann, R.W., Knoecklein, G.W. and Bonnell, C.H. (1994). Aeration of stratified lakes: Theory and practice. *Lake and Reserv. Manage.*, **8**, 99-120.

Little, J. C. (1995). Hypolimnetic aerators: Predicting oxygen transfer and hydrodynamics. *Wat. Res.*, **29**, 2475-2482.

McGinnis, D. F. and Little, J. C. (1998). Bubble dynamics and oxygen transfer in a Speece Cone. *Water Science & Technology*, **37** (2) 285-292.

McQueen, D.J. and Lean, D.R.S. (1986). Hypolimnetic aeration: An overview. *Water Poll. Res. J. Can*., **21**, 205-217.

Orsat, V., Vigneault, C. and Raghavan, G. S. V. (1993). Air Diffusers Characterization Using a Digitized Image Analysis System. *Applied Engineering in Agriculture,* **9**, 1, 115-121.

Schladow, S. G. (1993). Lake destratification by bubble-plume systems: Design methodology. *Jour. Hyd. Eng.*, **119**, 350-368.

Schwarzenbach, R.P., Gschwend, P. M. and Imboden, D.M. (1993). *Environmental Organic Chemistry*. John Wiley & Sons, Inc., New York.

Thomas, J.A., Funk, W.H., Moore, B.C. and Budd, W.W. (1994). Short term changes in Newman Lake following hypolimnetic aeration with Speece Cone. *Lake and Reserv. Manage*., **9**, 111-113.

Wüest, A., Brooks, N.H. and Imboden, D.M. (1992). Bubble plume modeling for lake restoration. *Wat. Resour. Res*., **28**, 3235-3250.

Table 1. Operating conditions for bubble-plume diffuser in Spring Hollow Reservoir.

Parameter	Value
Maximum depth [m]	55
Surface area [10^6 m^2]	0.4
Total water volume [10^6 m^3]	7.2
Active diffuser length [m]	360
Average diffuser depth [m]	43
Air flow rate [Nm^3 h^{-1}]	43

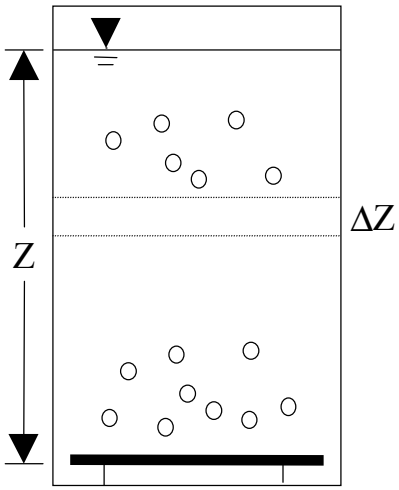

Figure 1. Schematic representation of bubbles rising in a well-mixed tank.

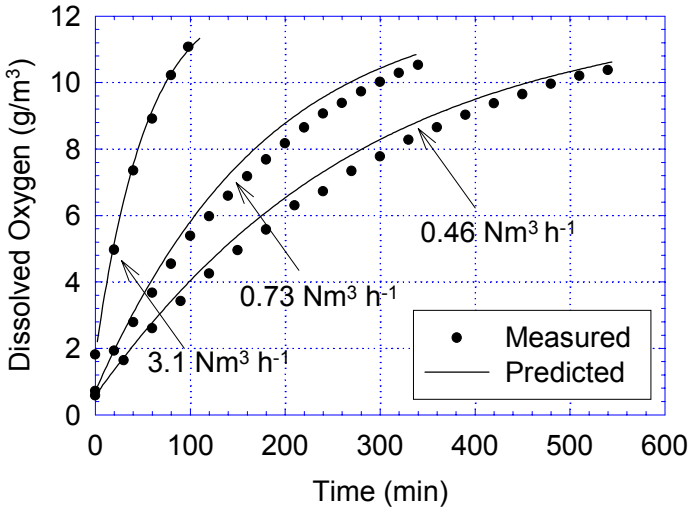

Figure 2. Observed and predicted oxygen concentrations in tank.

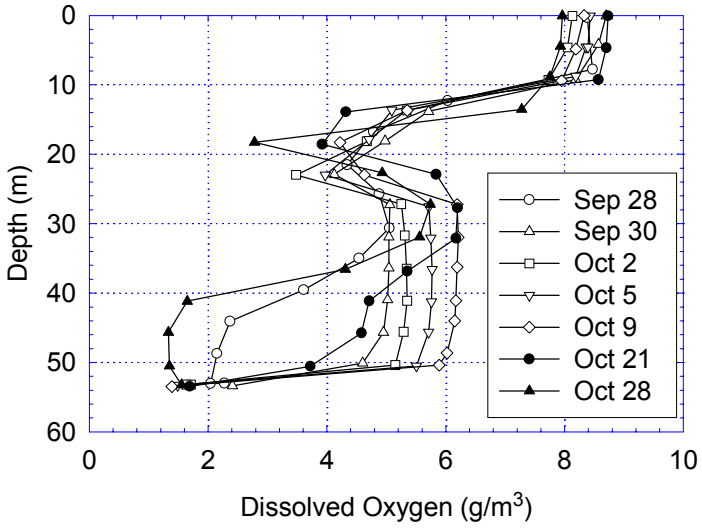

Figure 3. Observed oxygen profiles in Spring Hollow Reservoir.

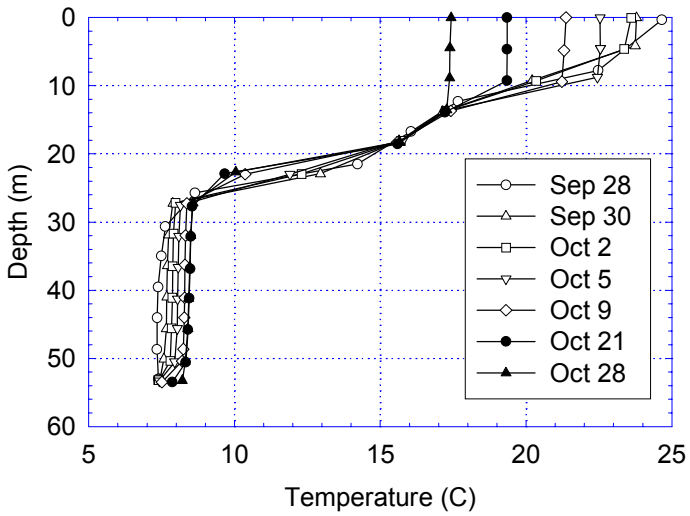

Figure 4. Observed temperature profiles in Spring Hollow Reservoir.

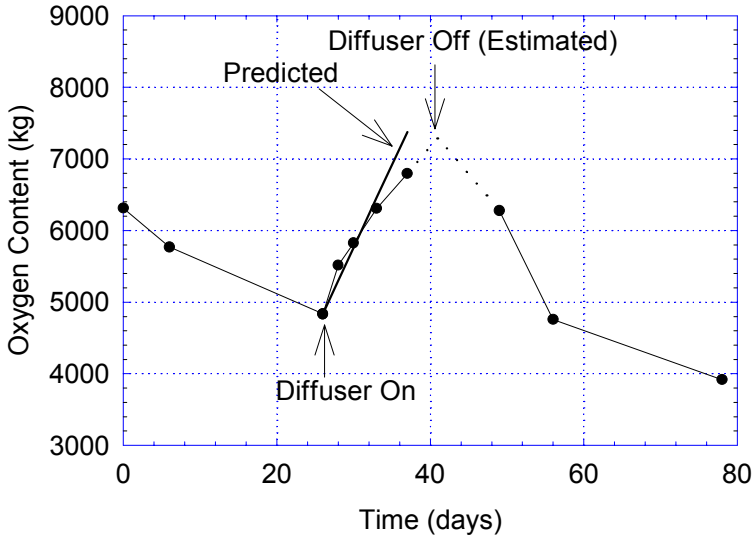

Figure 5. Measured and predicted hypolimnetic oxygen content in Spring Hollow Reservoir.

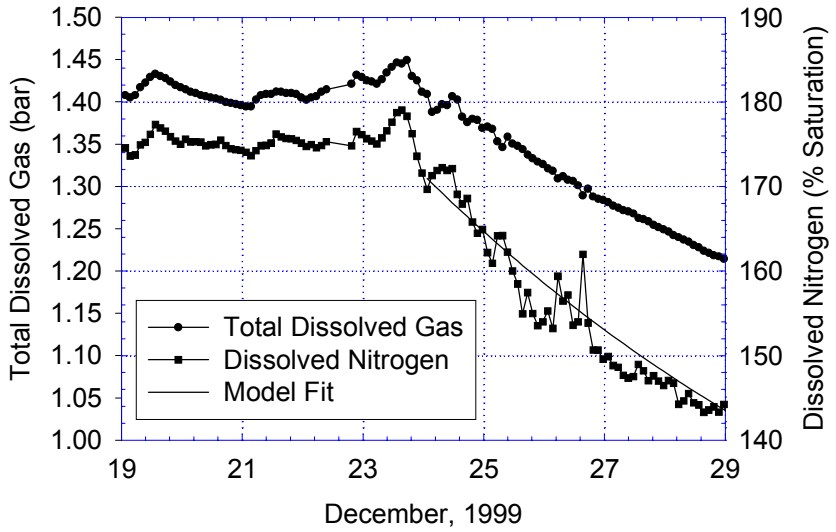

Figure 6. Dissolved nitrogen and total dissolved gas during destratification.

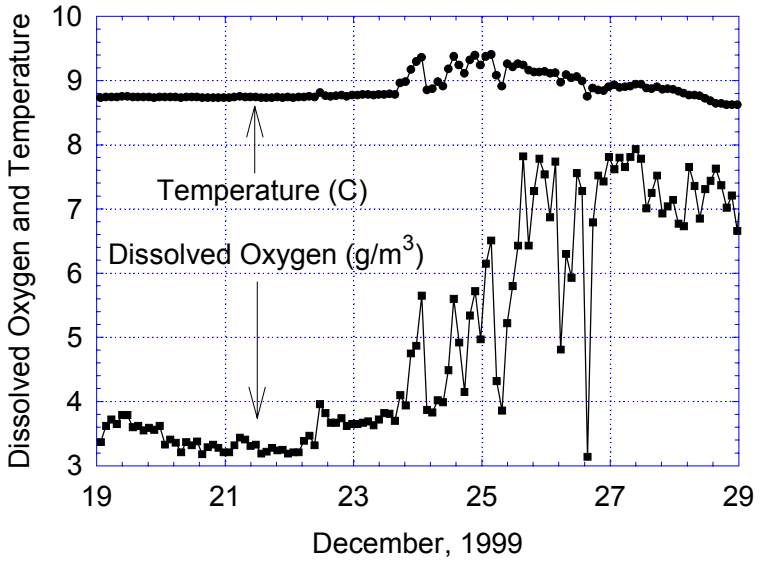

Figure 7. Dissolved oxygen and temperature during destratification.

VITA

Daniel Frank McGinnis was born on September 6, 1971 in Portsmouth, Virginia. He attended Tidewater Community College from 1991 – 1994 and received Associate of Science Degrees in Natural Science and in Engineering. Daniel then transferred to Virginia Tech and received his Bachelor of Science Degree in Civil Engineering with high honors. Daniel has since been employed part time as a technical specialist designing hypolimnetic oxygenation systems with Mobley Engineering, Inc. while completing his Master of Science Degree in Civil and Environmental Engineering.